The hornworts: morphology, evolution and development

Frangedakis, Eftychios ; Shimamura, Masaki ; Villarreal, Juan Carlos ; Li, Fay-Wei ; Tomaselli, Marta ; Waller, Manuel ; Sakakibara, Keiko ; Renzaglia, Karen S ; Szövényi, Péter

Abstract: Extant land plants consist of two deeply divergent groups, tracheophytes and bryophytes, which shared a common ancestor some 500 million years ago. While information about vascular plants and the two of the three lineages of bryophytes, the mosses and liverworts, is steadily accumulating, the biology of hornworts remains poorly explored. Yet, as the sister group to liverworts and mosses, hornworts are critical in understanding the evolution of key land plant traits. Until recently, there was no hornwort model species amenable to systematic experimental investigation, which hampered detailed insight into the molecular biology and genetics of this unique group of land plants. The emerging hornwort model species, Anthoceros agrestis, is instrumental in our efforts to better understand not only hornwort biology but also fundamental questions of land plant evolution. To this end, here we provide an overview of hornwort biology and current research on the model plant A. agrestis to highlight its potential in answering key questions of land plant biology and evolution.

DOI: https://doi.org/10.1111/nph.16874

New Phytologist

Review

Tansley review

The hornworts: morphology, evolution and development

Authors for correspondence:
Karen S. Renzaglia
Email: renzaglia@siu.edu
Péter Szövényi
Email: peter.szoevenyi@uzh.ch

Received: *17 April 2020*
Accepted: *28 July 2020*

Eftychios Frangedakis[1], Masaki Shimamura[2], Juan Carlos Villarreal[3,4], Fay-Wei Li[5,6], Marta Tomaselli[1], Manuel Waller[7], Keiko Sakakibara[8], Karen S. Renzaglia[9] and Péter Szövényi[7,10]

[1]Department of Plant Sciences, University of Cambridge, Cambridge, CB3 EA, UK; [2]Graduate School of Integrated Sciences for Life, Hiroshima University, Hiroshima 739-8528, Japan; [3]Department of Biology, Laval University, Quebec City, QC G1V 0A6, Canada; [4]Smithsonian Tropical Research Institute, Balboa, Ancon, Panamá; [5]Boyce Thompson Institute, Ithaca, NY 14853-1801, USA; [6]Plant Biology Section, Cornell University, Ithaca, NY 14853-1801, USA; [7]Department of Systematic and Evolutionary Botany, University of Zurich, Zurich 8008, Switzerland; [8]Department of Life Science, Rikkyo University, Tokyo 171-8501, Japan; [9]Department of Plant Biology, Southern Illinois University, Carbondale, IL 62901, USA; [10]Zurich-Basel Plant Science Center, Zurich 8092, Switzerland

Contents

New Phytologist (2021) **229:** 735–754
doi: 10.1111/nph.16874

Key words: *Anthoceros*, bryophytes, chloroplast, development, evolution, hornworts, symbiosis.

Summary

Extant land plants consist of two deeply divergent groups, tracheophytes and bryophytes, which shared a common ancestor some 500 million years ago. While information about vascular plants and the two of the three lineages of bryophytes, the mosses and liverworts, is steadily accumulating, the biology of hornworts remains poorly explored. Yet, as the sister group to liverworts and mosses, hornworts are critical in understanding the evolution of key land plant traits. Until recently, there was no hornwort model species amenable to systematic experimental investigation, which hampered detailed insight into the molecular biology and genetics of this unique group of land plants. The emerging hornwort model species, *Anthoceros agrestis*, is instrumental in our efforts to better understand not only hornwort biology but also fundamental questions of land plant evolution. To this end, here we provide an overview of hornwort biology and current research on the model plant *A. agrestis* to highlight its potential in answering key questions of land plant biology and evolution.

I. Introduction

Land plants (embryophytes) evolved from streptophyte algae (charophytes) some 500 million years ago (Delwiche & Cooper, 2015; Harholt *et al.*, 2016). The colonization of land by plants led to their diversification into the monophyletic group of bryophytes and the tracheophytes (vascular plants) (Renzaglia *et al.*, 2000; Nishiyama *et al.*, 2004; Leebens-Mack *et al.*, 2019). Bryophytes include liverworts, mosses and hornworts, while tracheophytes consist of lycophytes, ferns, gymnosperms and angiosperms. The

hornworts are the smallest and least diverse clade within bryophytes, consisting of *c.* 220 species (Söderström *et al.*, 2016) that are geographically widespread primarily in tropical areas (Villarreal *et al.*, 2014). Hornworts comprise the division Anthocerotophyta, the name of which is derived from three Greek words: άνθος/anthos (meaning flower), κέρας/ceras (meaning horn) and φυτό/phyto (meaning plant) and refers to the horn-like shape of the hornwort sporophyte (the multicellular diploid phase of the life cycle).

Inference about the common ancestor of land plants is ambiguous. This is, in part, due to the deep divergence of the three groups of bryophytes, as well as bryophytes and tracheophytes, that provided ample time for independent gains/losses of genes to occur. Comparison of the developmental, physiological and molecular features of hornworts with those of mosses and liverworts will provide a more accurate picture of the nature of the common ancestor of bryophytes and that of all land plants. It will also help to understand the diversity and molecular basis of evolution and development across bryophytes and tracheophytes.

Hornworts also possess a large number of unique traits that are not found in any other land plants. These include the following. (1) Zygote and sporophyte development: the orientation of the first zygote division is longitudinal, unlike in other land plants except leptosporangiate ferns (Johnson & Renzaglia, 2009). The sporophyte differs from mosses and liverworts in that it lacks a seta and continuously and progressively produces spores upwardly from a basal meristem, being essentially a growing sporangium. Sporophytes bear stomata, which may be homologous to those of tracheophytes (Renzaglia *et al.*, 2017; Harris *et al.*, 2020). (2) Chloroplast: it is the only extant land plant lineage, together with some lycophytes (Liu *et al.*, 2020), that has a single chloroplast (or just a few) per cell. The chloroplast of several hornwort species may contain a pyrenoid, a structure also found in many streptophyte algae and other algal lineages but not in other land plants (Li *et al.*, 2017; Meyer *et al.*, 2017). Hornwort plastid genomes have also one of the highest RNA editing rates amongst land plants (Small *et al.*, 2019) (3) Symbiosis: hornworts establish symbiotic relationships with endophytic cyanobacteria (Renzaglia *et al.*, 2009) and various fungal partners (mycorrhiza) (Desirò *et al.*, 2013). A small number of studies have provided insight into hornwort morphology and growth (Proskauer, 1948a,b; Renzaglia, 1978), but detailed molecular and genetic studies examining hornwort development are lacking.

Here, we review our current understanding of hornwort biology and development, highlighting the role that *Anthoceros agrestis* could play in shedding light on key innovations during land plant evolution.

II. The hornwort model species *Anthoceros agrestis*

First used by Micheli (1927) but properly designated by Linnaeus in 1753, *Anthoceros* L. was the first described and with 60 clearly delineated species (Söderström *et al.*, 2016), it is the most species-rich hornwort genus. *Anthoceros agrestis* Paton is emerging as the model system for the study of hornwort biology (Szövényi *et al.*, 2015). It is an annual species with a wide northern temperate distribution and has key features that make it amenable to laboratory study. This plant is small, easy to propagate, has a small genome size, and sexual reproduction is facilitated in the laboratory because the plants are monoicous (male and female reproductive organs are produced on the same individual) (Proskauer, 1948a,b; Szövényi *et al.*, 2015). *Anthoceros agrestis* has been adopted as a plant model by research groups around the world to study biological processes such as the evolution of circadian clocks (Linde *et al.*, 2017), microbial-type terpene synthase biochemistry (Xiong *et al.*, 2018) and RNA editing (Gerke *et al.*, 2019).

1. *Anthoceros agrestis* morphology and life cycle

Similar to all bryophytes, the life cycle of *A. agrestis* is dominated by the haploid gametophyte phase (Fig. 1). The gametophyte of *A. agrestis* is thalloid, often a rosette, with irregularly dissected margins and dorsal lamellae (Fig. 2a,b,d). The thallus lacks organized external appendages and specialized internal tissue differentiation except for mucilage canals (Fig. 2e) that form by separation between cells and *Nostoc* cavities that are colonized by cyanobacteria (Renzaglia *et al.*, 2009). Rhizoids develop on the ventral midline of the thallus (Fig. 2b,c). *A. agrestis* is monoicous, with male (antheridia) (Fig. 2h,f,g) and female (archegonia) (Fig. 2j,m) reproductive organs embedded in the thallus, differing from those in liverworts and mosses that are superficial. Antheridia are sunken in groups of 4–16 in chambers along the dorsal midline of the thallus. Each cluster of antheridia develops from a subepidermal cell in the apical notch (invaginated thallus margins where stem cells reside) (Campbell, 1918; Renzaglia *et al.*, 2009). The overlying epidermal cell forms the roof of the antheridial chamber that is two cells thick. Archegonia are also embedded in the thallus and they develop usually behind the growing point of the thallus. An archegonium is composed of neck canal cells and a ventral canal cell with an egg surrounded by thallus cells (Fig. 2j). When ready for fertilization, the neck canal cells and ventral canal cells disintegrate and the cover cells dissociate, leaving a canal for sperm cells to swim down to the egg (Fig. 2m). Antheridia typically develop and mature before archegonia. Similar to mosses, liverworts and lycophytes, fertilization takes place via biflagellate motile sperm (Fig. 2i) that swim to the egg via water and fuse, forming the diploid zygote. The embryo develops within the gametophyte and gives rise to the sporophyte (Figs 2d,k, 6a). Like other bryophytes, the hornwort sporophyte is matrotrophic, meaning it develops on and is nourished by the gametophyte. Unlike other plants, the sporophyte grows from a basal meristem that is established in the early stages of its development. The hornwort sporophyte is an elongated cylinder with no branching and, similar to most mosses, it possesses stomata (Fig. 2k,n). Sporogenous tissue is continually produced, meiosis is always occurring in a progressive and spatial (but not temporal) fashion, and all stages of spore differentiation are visible along the length of the sporophyte. There are no parallels to this development in any extant plant group or in the fossil record (Renzaglia *et al.*, 2000; Villarreal & Renzaglia, 2015). At maturity the sporophyte splits below the

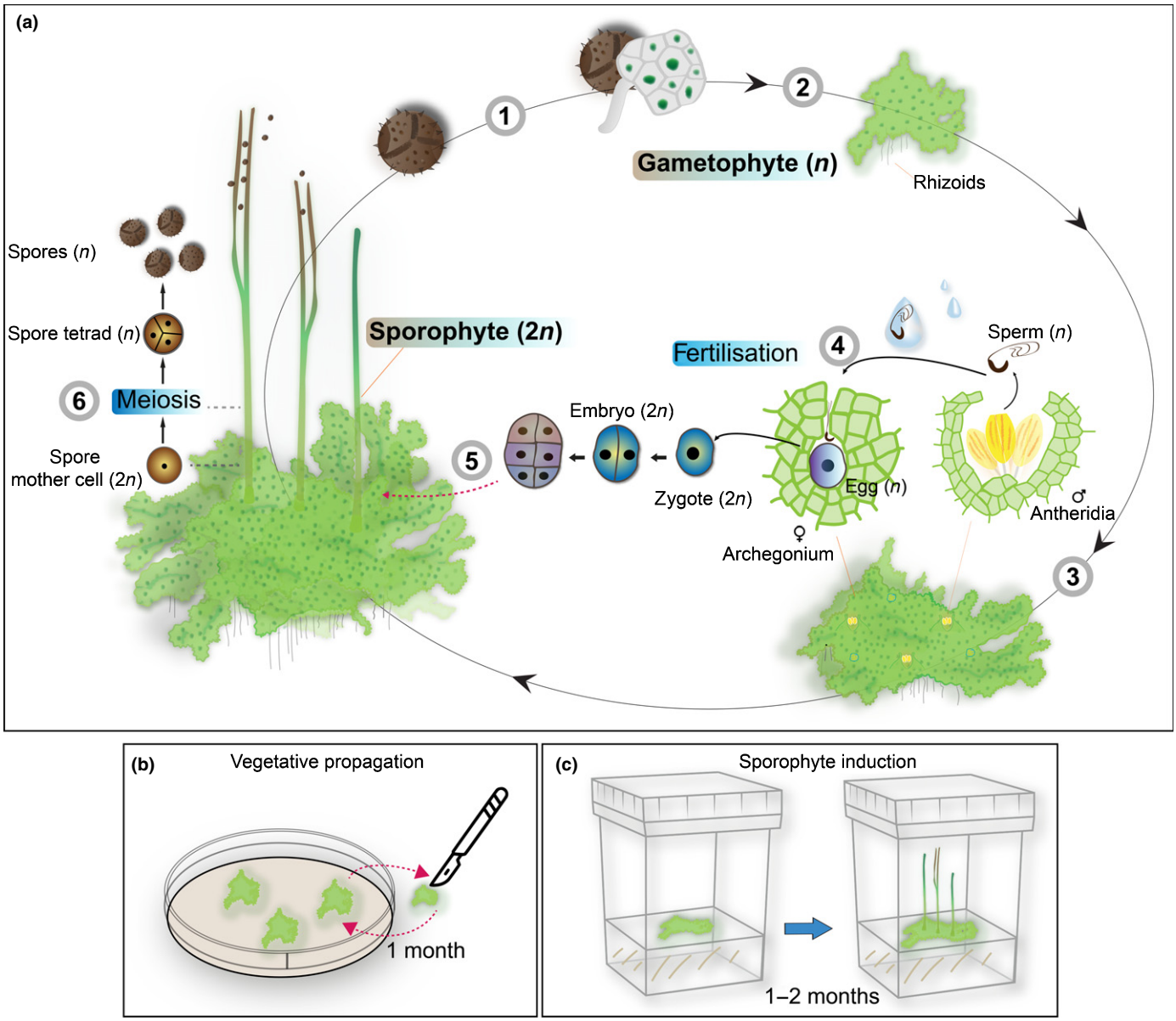

Fig. 1 Life and laboratory cycle of the hornwort *Anthoceros agrestis*. (a) *A. agrestis* has two life cycle phases: a dominant haploid phase called gametophyte and a diploid phase called sporophyte. The life cycle of *A. agrestis* starts with germination of the haploid spores (1) which develop into an irregularly shaped thallus (2). *A. agrestis* is monoicous, with both male and female reproductive organs present on the same individual. Male (antheridia) and female (archegonia) reproductive organs are embedded in the thallus and mitotically produce sperm and egg, respectively (3). Biflagellated motile sperm cells swim in water to the archegonium where the egg is fertilized (4). The resulting diploid zygote divides first by a longitudinal division and subsequent divisions to form the embryo, which is initially composed of three tiers. The bottom tier produces the foot. The middle tier gives rise to the basal meristem and the top tier forms the tip of the sporophyte (5). The sporophyte develops within the gametophyte and is nourished through the placenta, the junction between foot and gametophyte cells. Meiosis and sporogenesis occur progressively from the base of the sporophyte upwardly, leading to spore formation: sporogenous tissue at the base of the sporophyte produces spore mother cells that, via meiosis, produce spore tetrads and spores that are released at the tip where the sporophyte separates into two valves (6). *n*, haploid; 2*n*, diploid. (b, c) Laboratory cycle of *A. agrestis*. (b) Plants can be easily propagated in axenic culture by transferring small thallus fragments (typically 1 × 1 mm) onto plates with fresh growth media using sterile scalpels. (c) In laboratory conditions *A. agrestis* sporophyte induction can be achieved in 1–2 months under axenic conditions using a small thallus fragment as starting material.

apex and releases the spores (Fig. 2o). Spores germinate (Fig. 2a), typically resulting in a globose sporeling that forms an apical cell and develops into the thalloid gametophyte. Under low light conditions, the sporeling of *A. agrestis* forms a germ tube and has a short protonemal stage that is a single cell and produces the sporeling at its tip (Fig. 2a bottom) (Wada *et al.*, 1984).

2. *Anthoceros agrestis* laboratory cycle

A. agrestis plants are *c.* 0.5–1 cm in size in laboratory conditions, and can be maintained by vegetative (clonal) propagation under axenic conditions (Fig. 1b). There is no requirement for elaborate growth media or specialized growth facilities. Plants can routinely

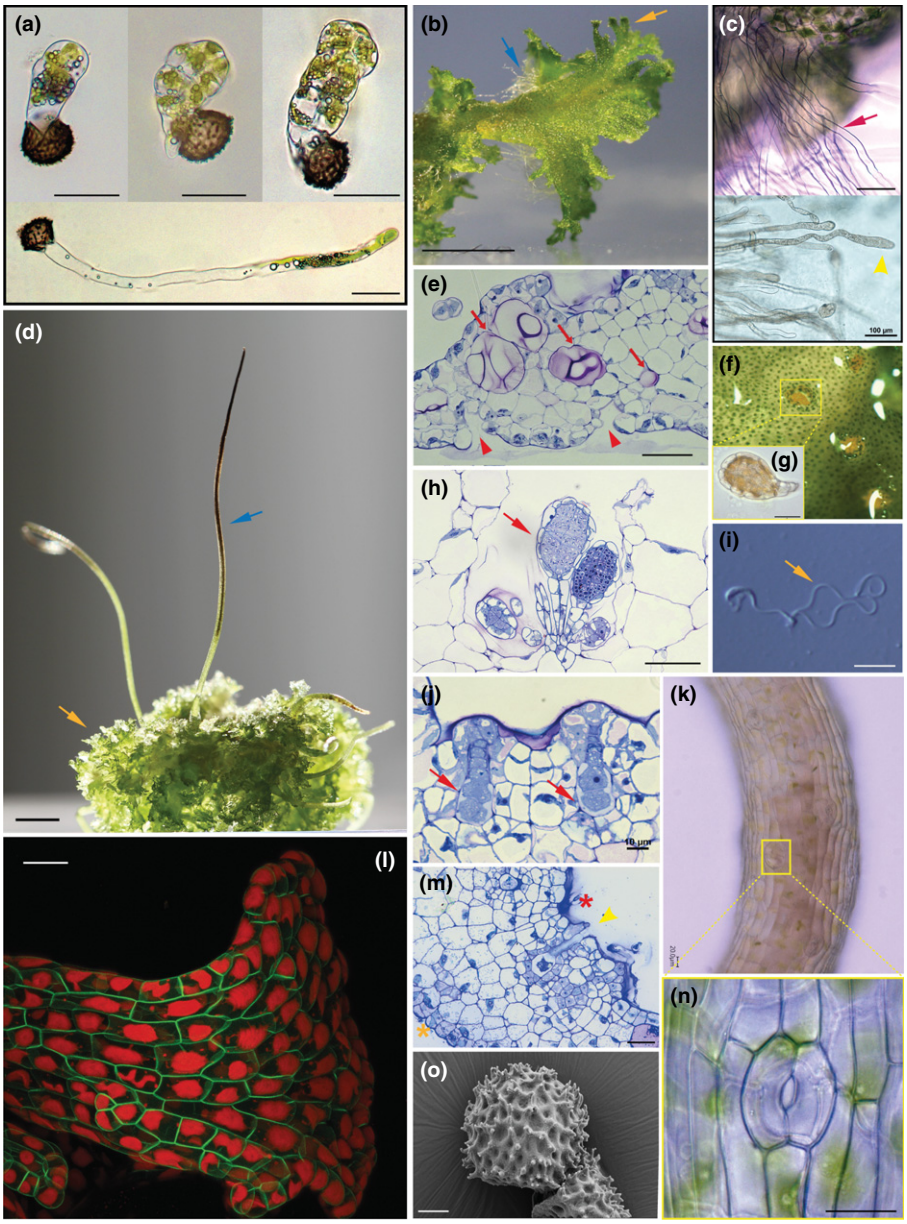

Fig. 2 Key morphological features of *Anthoceros agrestis*. (a) Light micrograph (LM) of germinating spores. Upper three images, successive stages in globose sporeling production. Lowermost: under low light conditions spore germination involves a germ tube, a long single-celled filament that develops a terminate globose sporeling. Bars, 50 μm. (b) Surface view of the irregularly shaped thallus. Blue arrow: rhizoids. Orange arrow: wavy thallus edge. Bar, 2.0 mm. (c) Top: LM of single-celled rhizoids on the ventral thallus (red arrow). Bar, 150 μm. Bottom: LM of single-celled rhizoid tips (yellow arrowhead) Bar, 100 μm. (d) Sporophytes (blue arrow) growing on the gametophyte (yellow arrow). Bar, 3.0 mm. (e) LM of longitudinal section of thallus with mucilage canals (red arrows). Mucilage clefts on the ventral side are indicated with red arrowheads. Bar, 50 μm. (h) LM of antheridia (red arrow) in an antheridial chamber in longitudinal section. Bar, 50 μm. (f) Surface view of antheridial chamber with yellow antheridia embedded in the dorsal thallus. Bar, 10 μm. (g) Antheridium removed from chamber in (f) showing antheridial body with sperm cells inside and stalk to the lower right. (h) LM of antheridia (red arrow) in an antheridial chamber in longitudinal section. Bar, 50 μm. (i) LM of biflagellate sperm. Coiled cell body is on the left and the flagella are on the right (yellow arrow). Bar, 5.0 μm. (j) LM of two archegonia embedded in the dorsal thallus in longitudinal section showing from the base up: egg cell, ventral canal cell, neck cells and cover cells. Bar, 10 μm. (k) Sporophyte with stomata. Bar, 20 μm. (l) Confocal fluorescence microscopy image of transgenic gametophyte showing single plastids in each cell. Green: green fluorescent protein localized in the plasma membrane expressed under the *CaMV* 35S promoter. Red, chlorophyll autofluorescence. Bar, 50 μm. (m) LM longitudinal section of thallus with an open archegonium (yellow arrowhead) containing only the egg cell near the apical notch. Dorsal side (red asterisk) and ventral side (orange asterisk). Bar, 25 μm. (n) Higher magnification LM of a stoma with two guard cells surrounding a pore. Bar, 10 μm. (o) Scanning electron micrograph of distal side of a spinose spore. Bar, 10 μm.

be propagated by transferring, on a monthly basis, small thallus fragments (usually 1 × 1 mm) on Petri dishes containing media with a source of nitrogen, potassium, calcium, magnesium and ferrous ions (such as BCD or 1/10 KNOP media; Szövényi *et al.*, 2015). Carbon source supplementation is not necessary, but addition of 2% (w/v) sucrose can enhance growth. Plants do not tolerate high light intensity (growth is optimal when light intensity is below 1500 lux), but photoperiod is not crucial with an

8 h : 16 h, light : dark regime being preferable. Two different isolates are currently available, the Oxford (originally from Scotland with cultures established at Oxford University) and the Bonn strain (originally from Germany). The conditions for successful induction of gametangia and subsequent sporophyte production have been determined (Szövényi *et al.*, 2015). The entire life cycle of *A. agrestis*, from spore to spore, can be completed within 3 months under laboratory conditions, which is similar to other established bryophyte model species such as the liverwort *Marchantia polymorpha*. Sporophyte induction is more efficient in the Bonn than in the Oxford isolate. It can be achieved by transferring plants (thallus) grown for 1 month at 22–16°C under an 8 h : 16 h, light : dark photoperiod regime. Approximately 1 month later antheridia produced in the thallus are visible as yellow–orange spots. For fertilization, the addition of water on the thallus is necessary. Sporophytes develop after an additional month (Fig. 1c). Protocols for DNA and RNA extraction are also available despite hornworts appearing to have high polysaccharide and polyphenol content, which usually make nucleic acid extraction challenging. Finally, a simple *Agrobacterium*-mediated transformation technique is currently under optimization, with fluorescent proteins such as the green fluorescent protein (GFP) being successfully expressed in *A. agrestis* plants (Fig. 2l). The tissue used for transformation is the haploid thallus, and thus there is no need for crosses to establish inbred lines like in many tracheophyte plant model systems.

3. *Anthoceros agrestis* genome

The genomes of the two *A. agrestis* isolates have been sequenced (Li *et al.*, 2020) and a high-quality genome assembly has been generated with an estimated genome size of 126.1 Mb (Oxford isolate) and 124.5 Mb (Bonn isolate), amongst the smallest in land plants (Bowman *et al.*, 2017; Pellicer *et al.*, 2018). The number of predicted protein-coding genes varies between 24 700 and 25 800 with an estimated chromosome number of six (Li *et al.*, 2020). There is no evidence of whole-genome duplication but 36–38% of the genome is estimated to be composed of repetitive and transposable elements, with the most abundant being long terminal repeat (LTR) retrotransposons. A whole genome assembly is also available for *Anthoceros punctatus* (Li *et al.*, 2020) and *Anthoceros angustus* (Zhang *et al.*, 2020). The *A. punctatus* genome is about 10–20 Mb larger than the *A. agrestis* genomes mainly due to repeat expansions. Nevertheless, the *A. agrestis* and *A. punctatus* genomes are largely collinear with a very similar gene complement, while fewer genes were predicted for *A. angustus*. Hornworts also have the smallest set of transcription-associated proteins (TAPs) (Wilhelmsson *et al.*, 2017) among all land plant groups sequenced to date. Therefore, the *A. agrestis* represents an appropriate model system for genetic studies owing to its small and paralog poor genome.

III. Phylogeny of land plants and hornworts

The monophyly of tracheophytes (lycophytes, ferns, gymnosperms and angiosperms) is well supported, while the interrelationships among bryophyte lineages and tracheophytes have been the subject of a long-standing debate (Nishiyama *et al.*, 2004; Qiu *et al.*, 2006; Wickett *et al.*, 2014; Morris *et al.*, 2018).

Until recently the widely accepted hypothesis was that bryophytes are paraphyletic, with liverworts, mosses and hornworts being successive sister lineages to tracheophytes (Qiu *et al.*, 2006) (Fig. 3a). However, several recent phylogenomic studies have challenged this view. In particular, the monophyly of liverworts and mosses (Setaphyta) is well supported, with hornworts either sister to Setaphyta (i.e. bryophyte monophyly) or to all land plants (Renzaglia *et al.*, 2000, 2018; Morris *et al.*, 2018) (Fig. 3b,c). The monophyly of bryophytes was further supported by the analysis of over 1000 plant transcriptomes (Leebens-Mack *et al.*, 2019) and by three more studies using whole genome information (Harris *et al.*, 2020; Li *et al.*, 2020; Zhang *et al.*, 2020). Therefore, there is mounting evidence that extant bryophytes are monophyletic, with hornworts sister to a moss and liverwort clade (Fig. 3c). The above-mentioned analyses rejected the hypothesis that liverworts are sister to all other extant land plant lineages as proposed by Qiu *et al.* (2006).

By contrast, hornwort phylogeny is less controversial. Traditionally, a series of morphological characters were used for resolving hornwort phylogenies: thallus shape, chloroplast number per cell, presence and morphology of pyrenoid, stomata and colour of the spore wall (Cargill *et al.*, 2005). Several recent molecular analyses have provided more robust insight into hornwort phylogenetic relationships and pointed to the limitations of morphological characters in clarifying relationships (Duff *et al.*, 2007; Villarreal & Renner, 2012, 2013). Hornworts comprise 11 genera: *Leiosporoceros*, *Anthoceros*, *Folioceros*, *Paraphymatoceros*, *Phaeoceros*, *Notothylas*, *Phymatoceros*, *Phaeomegaceros*, *Nothoceros*, *Megaceros* and *Dendroceros*, that are placed into five orders: Leiosporocerotales, Anthocerotales, Notothyladales, Phymatocerotales and Dendrocerotales (Fig. 3d) (Villarreal & Renner, 2012). *Leiosporoceros* is sister to all other hornworts and the Anthocerotaceae, which includes *Anthoceros* and *Folioceros*, is sister to the remaining taxa (Söderström *et al.*, 2016). A single and recent (< 1 million years ago (Ma)) origin of the European *A. agrestis* has been suggested (Dawes *et al.*, 2020) (Fig. 3e).

IV. Hornwort development

All extant representatives of streptophyte algae, the sister group to land plants, possess a haplontic life cycle in which mitotic divisions are restricted to the haploid phase that produces gametes and the diploid phase is represented by a single cell (zygote) undergoing meiosis. By contrast, mitotic divisions occur in both haploid and diploid phases of all land plants leading to the alternation of multicellular haploid and multicellular diploid phases, referred to as a haplodiplontic life cycle. In contrast to the dominant gametophyte and dependent sporophyte in bryophytes, the free-living sporophyte in tracheophytes has progressively increased in complexity, with the gametophyte reduced to just a few cells in seed plants. In flowering plants, the male and female gametophytes are represented by the pollen and the embryo sac, respectively (Niklas & Kutschera, 2009).

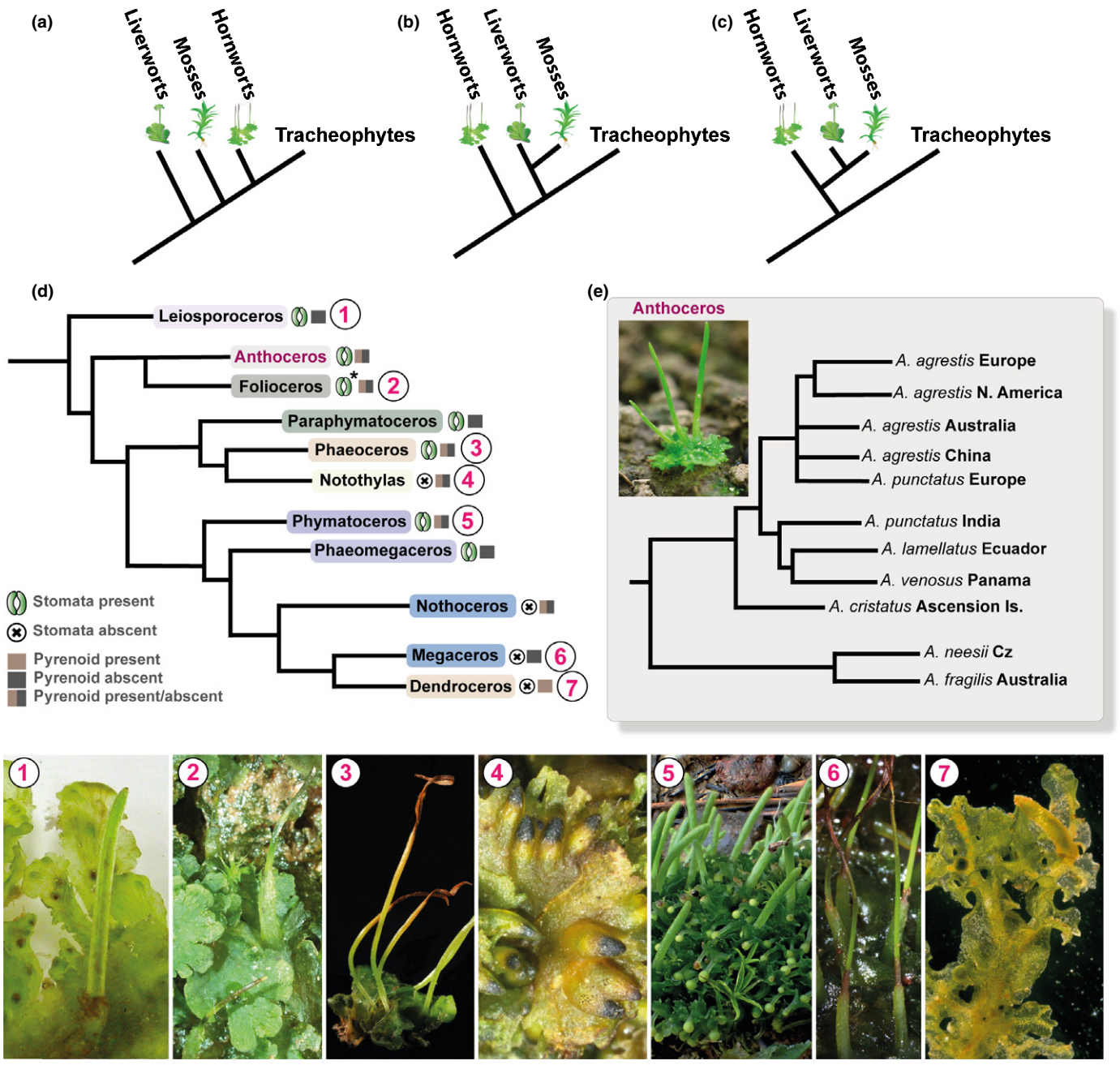

Fig. 3 Phylogeny of land plants and hornworts. (a–c) Competing hypotheses about the phylogenetic position of hornworts among land plants. (a) Liverworts, mosses and hornworts are successive sister lineages to tracheophytes (Qiu *et al*., 2006). (b) Hornworts are sister to all other land plants with liverworts and mosses monophyletic (Wickett *et al*., 2014). (c) Monophyletic bryophytes with hornworts sister to Setaphyta that include mosses and liverworts (Renzaglia *et al*., 2018; Li *et al*., 2020). (d) Phylogeny of hornworts based on Villarreal & Renner (2012); numbered circles next to the names in the phylogenetic tree correspond to species example images below. *Phaeoceros* photo credit: John Baker, University of Oxford (2020). The presence and/or absence of stomata and pyrenoid is indicated next to each genera name. *Exception: stomata absent in *Folioceros incurvus* (Renzaglia *et al*., 2009; Villarreal & Renner, 2012). (e) Phylogeny of the *Anthoceros agrestis*/*Anthoceros punctatus* group based on Dawes *et al*. (2020).

Because all extant taxa of streptophyte algae are haplontic, it is assumed that the origin of the haplodiplontic life cycle and that of the multicellular sporophyte phase are tightly linked to the evolution of land plants (Langdale, 2008; Bowman *et al*., 2016; Kenrick, 2018). The land plant sporophyte has undergone major morphological and physiological changes during evolution (Harrison, 2017; Szövényi *et al*., 2019). In the bryophyte lineage this generation is developmentally simple and unbranched while in the tracheophyte lineage it is a highly variable and often elaborate plant body with a wide array of organs and tissue systems. Because hornworts are sister to Setaphyta and sporophytic features of the three bryophyte clades are highly divergent, hornworts are key to revealing shared sporophytic characters with Setaphyta, and thereby provide information on the sporophytic complexity of

the common ancestor of bryophytes. Moreover, hornworts are critical to better understand the evolutionary mechanisms leading to the increased complexity and dominance of the sporophytic phase in tracheophytes (Villarreal & Renzaglia, 2015). To facilitate future evolutionary studies focused on early land plants, we describe the anatomy and development of the hornwort gametophyte and sporophyte phases in the sections that follow. Comparisons are made with the model liverwort *M. polymorpha* and the model moss *Physcomitrium patens* (formerly *Physcomitrella patens)*, and our current understanding of the genetic control of development in these plants is discussed.

1. Gametophyte

In the *A. agrestis* gametophyte there are multiple wedge-shaped apical cells (stem cells) with four cutting faces in notches around the thallus (Fig. 4). Derivatives from the apical cells divide and form a flattened orbicular gametophyte with clearly defined dorsal and ventral sides (Renzaglia, 1978) and wavy margins. Dorsal derivatives give rise to the gametangia (Fig. 2h,m) and upper thallus while ventral derivatives form the rhizoids, *Nostoc* cavities and lower thallus region (Figs 2c,e, 8). Lateral derivatives produce tissue that 'fuses' adjacent growing notches forming the rosette. In the model liverwort *M. polymorpha* the thallus has a single apical notch (or two if branching), and basal (ventral and dorsal) derivatives divide more than the two lateral derivatives, making the thallus to elongate and form a dichotomously branched strap-shaped gametophyte (Shimamura, 2016).

In the model moss *P. patens*, gametophyte development involves the production of filamentous protonemata directly from germinating spores. Protonemata grow from their tips, and side-branch initial cells differentiate into buds that develop single tetrahedral apical cells that divide to produce leafy shoots called gametophores (Kofuji & Hasebe, 2014). Each derivative from the three cutting faces of the apical cell produces a leaflet giving rise to the spiralled arrangement of leaflets on the gametophore (Renzaglia *et al.*, 2018).

Several studies have attempted to shed light on gametophytic growth of bryophytes by focusing on the role of *CLAVATA3/EMBRYO SURROUNDING REGION-related* (*CLE*) and *CLAVATA1* (*CLV1*) genes. *CLE* genes are found in all land plants studied (but not in charophytes) (Fig. 5) and can be categorized into two major subclasses: *TRACHEARY ELEMENT DIFFERENTIATION INHIBITORY FACTOR*-like (*TDIF*-like) and *CLAVATA3*-like (*CLV3*-like) (Hirakawa & Bowman, 2015; Hirakawa & Sawa, 2019). *TDIF*-like peptides regulate stem cell maintenance in the vasculature (Hirakawa *et al.*, 2008) while *CLV3*-like peptides control stem cell maintenance in the shoot apical meristem (SAM) and partly in the root meristem (Barton, 2010; Kim *et al.*, 2017). *TDIF* and *CLV3* act via receptors: *TRACHEARY ELEMENT DIFFERENTIATION INHIBITORY FACTOR RECEPTOR* (*TDR)* for *TDIF* and *CLAVATA1* for *CLV3* (Hirakawa & Sawa, 2019).

The genome of *M. polymorpha* has two *CLE* homologues, *MpCLE1/TDIF* and *MpCLE2/CLV3*, as well as homologues of their respective receptors, *MpTDR* and *MpCLV1*. *MpCLE1* and its receptor gene *MpTDR* are expressed in distinct patterns across the gametophyte apical notch and act as a negative regulator of gametophytic apical cell meristematic activity (Hirakawa *et al.*, 2019). In the moss *P. patens*, there are nine (Goad *et al.*, 2017; Whitewoods *et al.*, 2018; Whitewoods, 2020) potential *CLE* genes (Fig. 5) and two *CLV1* genes. All *CLE* genes belong to the *CLV3*-like subclass while genes of the *TDIF*-like subclass are absent. Three *CLE* genes and their receptors *PpCLV1a*, *PpCLV1b* and *PpRPK2* are co-expressed in the gametophyte shoot regulating orientation of stem cell division planes during the transition from two- to three-dimensional growth in the gametophyte (Whitewoods *et al.*, 2018).

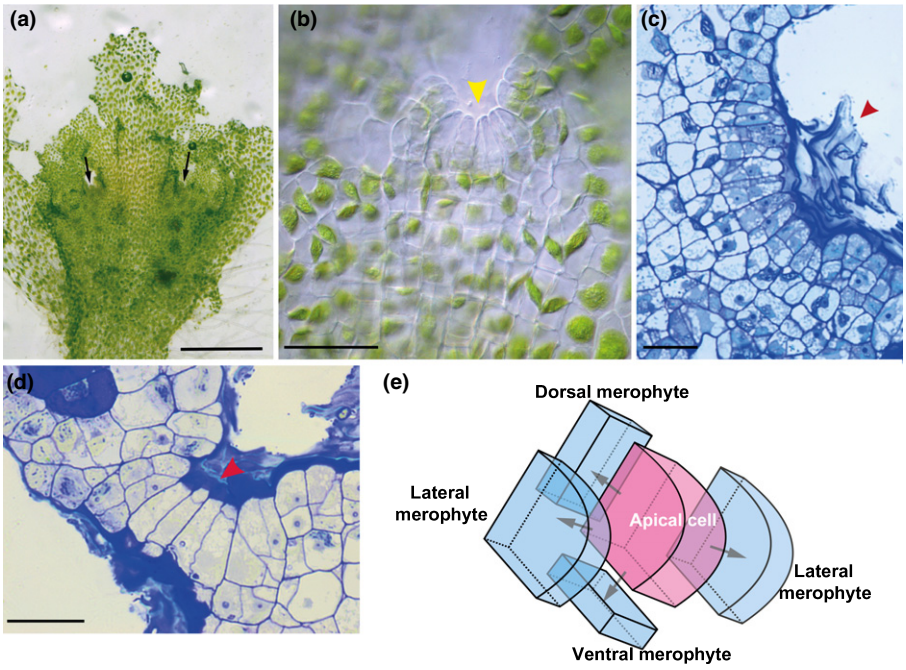

Fig. 4 *Anthoceros agrestis* gametophyte apical growth. (a) Surface view of *A. agrestis* gametophyte. Arrows indicate apical notches. Bar, 1.0 mm. (b) Light microscopy (LM) surface view of apical notch (yellow arrowhead) showing row of apical cell and immediate derivatives and single chloroplasts in older cells. Bar, 50 μm. (c) LM surface section of apical notch covered by mucilage (red arrowhead). Bar, 50 μm. (d) LM transverse section of thallus showing four rectangular cells that include the apical cell (red arrowhead) and three immediate derivatives in a growing notch covered by mucilage. The more abundant cells on either side are from divisions in the lateral derivatives. Bar, 50 μm. (e) Schematic representation of gametophyte apical cell (pink) with four cutting faces and four derivatives (blue).

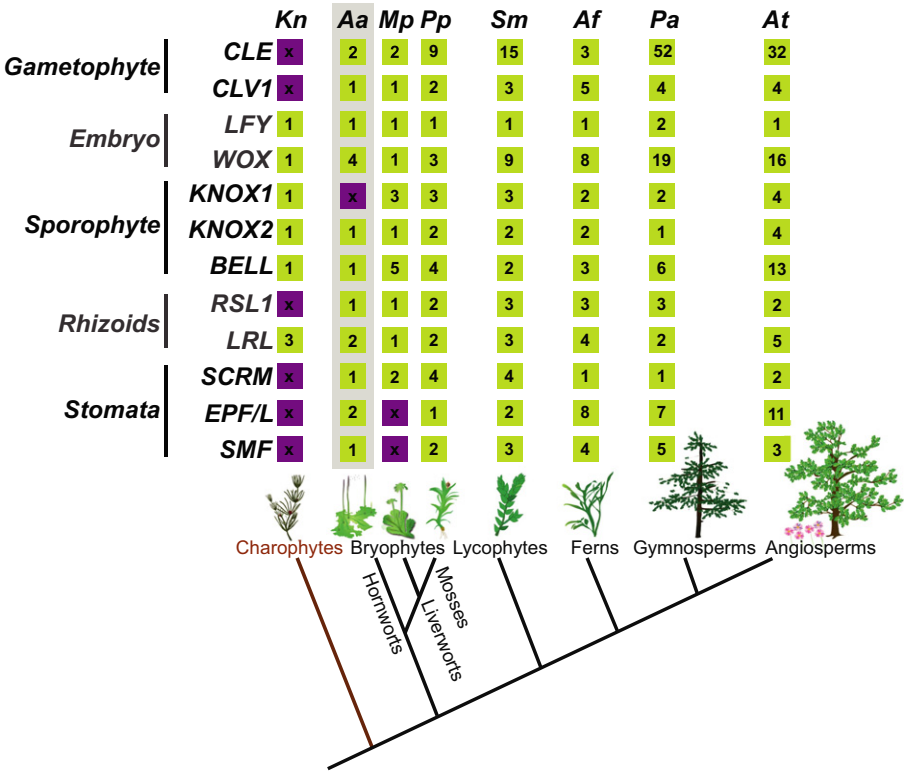

Fig. 5 Key developmental genes of land plants. Key genes controlling gametophyte, embryo, sporophyte, rhizoid and stomata development in bryophytes. Bottom: phylogenetic relationships of the major lineages of land plants illustrating the monophyly of bryophytes, lycophytes, ferns, gymnosperms and angiosperms (tracheophytes) (Li *et al*., 2020). *CLE*, refers to the number of *CLE* signalling peptide-encoding genes. Kn, *Klebsormidium nitens*; Aa, *Anthoceros agrestis*; Mp, *Marchantia polymorpha*; Pp, *Physcomitrium (Physcomitrella) patens*; Sm, *Selaginella moellendorffii*; Af, *Azolla filiculoides*; Pa, *Picea abies*; At, *Arabidopsis thaliana*. Numbers in yellow boxes indicate the number of homologues in the corresponding species genome. Purple boxes with 'x' indicate the absence of the homologue (Miwa *et al*., 2009; Nystedt *et al*., 2013; Bowman *et al*., 2017; Li *et al*., 2018, 2020; Whitewoods *et al*., 2018; Zhang *et al*., 2020).

The role of *CLV1* in regulating cell division plane orientation in *P. patens* has been shown to be shared with *Arabidopsis thaliana* but not with *M. polymorpha*. *A. agrestis* has one *TDIF*-like and one CLE-encoding gene and a single *CLV1* (Fig. 5) and it can be speculated that they may play a role in gametophyte growth regulation similar to other bryophytes.

Additional genes seem to be part of the network regulating apical cell development in *P. patens*, such as the *DEFECTIVE KERNEL 1* (*DEK1*) (Perroud *et al*., 2020) and the *NO GAMETOPHORES 1* (*NOG1*) (Moody *et al*., 2018), and genes encoding polycomb group (PcG) and PIN proteins (Bennett *et al*., 2014). For example, the *P. patens Fertilization Independent Endosperm* (*PpFIE*) gene, which encodes a PcG protein, is expressed only in the gametophyte apical cells and in cells that undergo fate transition. In the absence of *PpFIE*, gametophore meristems overproliferate but also fail to further develop and reach the reproductive phase. This illustrates the key role of *PpFIE* in the regulation of differentiation and proliferation of gametophytic stem cells in *P. patens* (Mosquna *et al*., 2009). Similar observations were made on knockouts involving the *P. patens* CURLY LEAF (CLF), another PcG protein (Okano *et al*., 2009). *A. agrestis* has homologues of *NOG1*, *DEK1*, *PpCLF* and *PpFIE* (Li *et al*., 2020). To what extent these genes are also involved in the regulation of gametophyte apical growth in *A. agrestis* needs to be confirmed by functional studies.

2. Rhizoids

Tracheophytes have specialized, complex multicellular structures on the sporophyte called roots that are involved in water and nutrient uptake, anchoring the plant to a substrate and mediating symbiosis (Jones & Dolan, 2012). Roots have outgrowths of epidermal cells called root hairs that effectively increase the total surface area for water absorption. Bryophytes, by contrast, lack roots and have instead simple tip-growing filamentous cells, called rhizoids (Fig. 2b,c) which are unicellular in hornworts and liverworts but multicellular in mosses. Rhizoids and root hairs serve a similar function, allowing nutrient absorption from the soil and anchorage (Jones & Dolan, 2012). In all bryophytes including hornworts, rhizoid development is restricted to the gametophyte. All hornworts have unbranched rhizoids with the exception of *Megaceros* and *Nothoceros* in which rhizoids branch at the tip (Renzaglia, 1978).

Class 1 *ROOT HAIR DEFECTIVE SIX-LIKE* (*RSL*) genes regulate root hair development in the sporophyte of *A. thaliana* and rhizoid development in the gametophyte of the bryophytes *M. polymorpha* and *P. patens* (Menand *et al*., 2007; Catarino *et al*., 2016; Proust *et al*., 2016). Similarly, *LOTUS JAPONICUS ROOTHAIRLESS1-LIKE* (*LRL*) group XI basic helix–loop–helix (bHLH) transcription factors also play a key role in the regulation of root hair and rhizoid development in *M. polymorpha*, *P. patens* and *A. thaliana* (Tam *et al*., 2015).

RSL–LRL genetic networks have been repeatedly deployed to control rhizoid or root hair development in different land plant groups during evolution. *A. agrestis* has a single class 1 *RSL* homologue and two *RLR* homologues (Fig. 5). It is very likely that the same set of genes regulate rhizoid development in *A. agrestis*. It must be noted, however, that not all elements of the genetic network that controls rhizoid development are likely to be conserved. FEW RHIZOIDS1 (MpFRH1), a microRNA that acts as a negative regulator of the class 1 RSL gene in *M. polymorpha*,

has recently been identified (Honkanen *et al.*, 2018; Thamm *et al.*, 2020). This demonstrated that the negative regulators of class 1 RSL genes, at least in liverworts, are different from those in *A. thaliana* where class 1 RSL genes are negatively regulated by a Class IV homeodomain-leucine-zipper protein, AtGL2 (Di Cristina *et al.*, 1996; Bernhardt *et al.*, 2003; Lin *et al.*, 2015).

3. Embryo

In hornworts, after fertilization the first division of the zygote is parallel to the longitudinal axis of the archegonium (Fig. 6a) (Renzaglia, 1978). This is unlike other bryophytes in which the initial division is transversal. Leptosporangiate ferns also have longitudinal first divisions in the zygote and this may be related to hornworts and ferns having zygotes and embryos in an embedded archegonium (Shaw & Renzaglia, 2004; Johnson & Renzaglia, 2009). Subsequent divisions give rise to the embryo, which is composed of three tiers (Fig. 1a) (Ligrone *et al.*, 2012). The first (lowest) tier produces the foot early in development of the sporophyte. The second (middle) tier gives rise to the meristematic area of the sporophyte, referred to as the basal meristem. Finally, the third (top) tier gives rise to the tip of the sporophyte capsule. The first- and the third-tier cells stop dividing early in sporophyte development.

In *P. patens FLORICAULA/LEAFY* (*FLO*/*LFY)* is required for the first cell division in the zygote (Maizel *et al.*, 2005; Tanahashi *et al.*, 2005). *Physcomitrella patens* has two *LFY* genes, *PpLFY1* and *PpLFY2* (Tanahashi *et al.*, 2005), and in loss-of-function mutants the zygote nucleus does not divide after fertilization. Notably, *P. patens LFY* does not complement *LFY* mutants in *A. thaliana*, indicating that LFY function in angiosperms has diverged from that in bryophytes (Tanahashi *et al.*, 2005). It has been demonstrated that these differences in LFY function can be attributed to specific amino acid substitutions in the DNA binding domain of the LFY protein (Maizel *et al.*, 2005). *A. agrestis* has a single *LFY* homologue (Fig. 5) and its expression seems to be more pronounced in the gametophyte stages (Li *et al.*, 2020) unlike the predominantly sporophytic expression in *P. patens*. Future functional analysis will elucidate its potential role in embryo development in hornworts.

WUS-related homeobox (*WOX*) genes (Haecker *et al.*, 2004) regulate key aspects of plant development, such as stem cell maintenance (Laux *et al.*, 1996; Kamiya *et al.*, 2003; Hirakawa *et al.*, 2010), and zygote and embryo development (Breuninger *et al.*, 2008; Ueda *et al.*, 2011). *WOX* genes can be grouped into three subclasses (Zhang *et al.*, 2017; Wu *et al.*, 2019): the *WUSCHEL* (*WUS*) clade, *WOX9* clade and *WOX13* clade. All *WOX* genes in the *P. patens* genome belong to the *WOX13* clade (van der Graaff *et al.*, 2009). *Physcomitrella patens* zygotes lacking activity of the two *WOX13*-like genes are unable to elongate and initiate the apical cell of the embryo (Sakakibara *et al.*, 2014). This function is different from the *A. thaliana WOX13* gene, which promotes replum formation in the fruit (Romera-Branchat *et al.*, 2013), and *WOX14*, which promotes vascular cell differentiation (Denis *et al.*, 2017). The *A. agrestis* genome has four *WOX13* clade members (Fig. 5). *WOX13-like 1* is specifically expressed in sporophytes while *WOX13-like 2*, *3* and *4* are expressed in both the gametophyte and the sporophyte (Li *et al.*, 2020) and may have diverse roles in stem cell maintenance and embryo development.

4. Sporophyte

A single gametophyte thallus can produce multiple sporophytes (Fig. 2d). Similar to other bryophyte groups the hornwort sporophyte is largely dependent on the gametophyte (Renzaglia *et al.*, 2000). The *A. agrestis* sporophyte grows from a basal meristem (Fig. 6b–d) that continuously produces new sporophytic tissue upwardly and eventually gives rise to spores and pseudoelaters. Spores mature progressively from the bottom to the top of the sporophyte. The basal meristem remains active throughout the entire life of the sporophyte (Renzaglia *et al.*, 2009). At maturity, the sporophyte is composed of (from the centre to the outer layer) (Fig. 6c): the columella, sporogenous tissue, assimilative (photosynthetic) tissue and epidermis. The columella is important in spore dispersal and is composed of 16 cells that are living until sporophyte dehiscence (Fig. 6c,f,g). From the basal meristem (Fig. 6d), two layers of cells begin to differentiate between the columella and assimilative tissue, forming the archesporium that gives rise to the sporogenous tissue, including spore mother cells and sterile pseudoelaters (Fig. 6c,f,h,m). Sporogenesis begins with the differentiation and enlargement of rounded spore mother cells (Fig. 6c) that undergo meiosis and develop into the spores (Fig. 6j, k,h). Pseudoelaters are interspersed among sporogenous cells; they are multicellular and do not undergo meiosis (Fig. 6c,m). Spore maturation involves the development of a three-layered spore wall (Fig. 6l) that consists of a thin outer layer followed by a thick inner layer with globular sporopollenin (called outer and inner exine respectively), and an innermost layer (called intine) similar to the primary cell wall in composition except that it contains callose (Renzaglia al., 2020). The proximal spore surface (where spores of the tetrad meet) has an aperture with thickened intine, which is the site of germination (Fig. 6j,k,l). Spore tetrads are surrounded by the spore mother cell wall until late in development when all wall layers are compacted (Fig. 6l). Storage material in the spores consists of protein and oils (Fig. 6l).

The basis of the sporophyte is surrounded by gametophytic tissue called involucre (Fig. 6b,c) and is anchored in the gametophyte by the bulbous foot that contains peripheral cells (called haustorial cells) that elongate into gametophytic cells forming the placenta (Fig. 6d,e). Unlike the vast majority of land plants, cell-wall ingrowths typical of transfer cells in hornworts are restricted to gametophyte cells of the placenta (Fig. 6d,e). Sporophyte haustorial cells have thin smooth walls and penetrate the surrounding gametophytic tissue, allowing efficient transfer of nutrients from the gametophyte to the sporophyte (Fig. 6d,e; Ligrone & Renzaglia, 1990).

In *P. patens* the sporophyte initially grows from an apical cell that forms in the first few cell divisions of the embryo, but apical cell activity ceases after *c.* 12 cell divisions (Sakakibara *et al.*, 2008). A new multicellular meristem, called the intercalary or seta meristem, is then formed in the middle of the sporophyte (Sakakibara *et al.*, 2008). Meristematic activity of the seta meristem terminates and is followed by expansion of the sporangium or capsule. The

Colour online

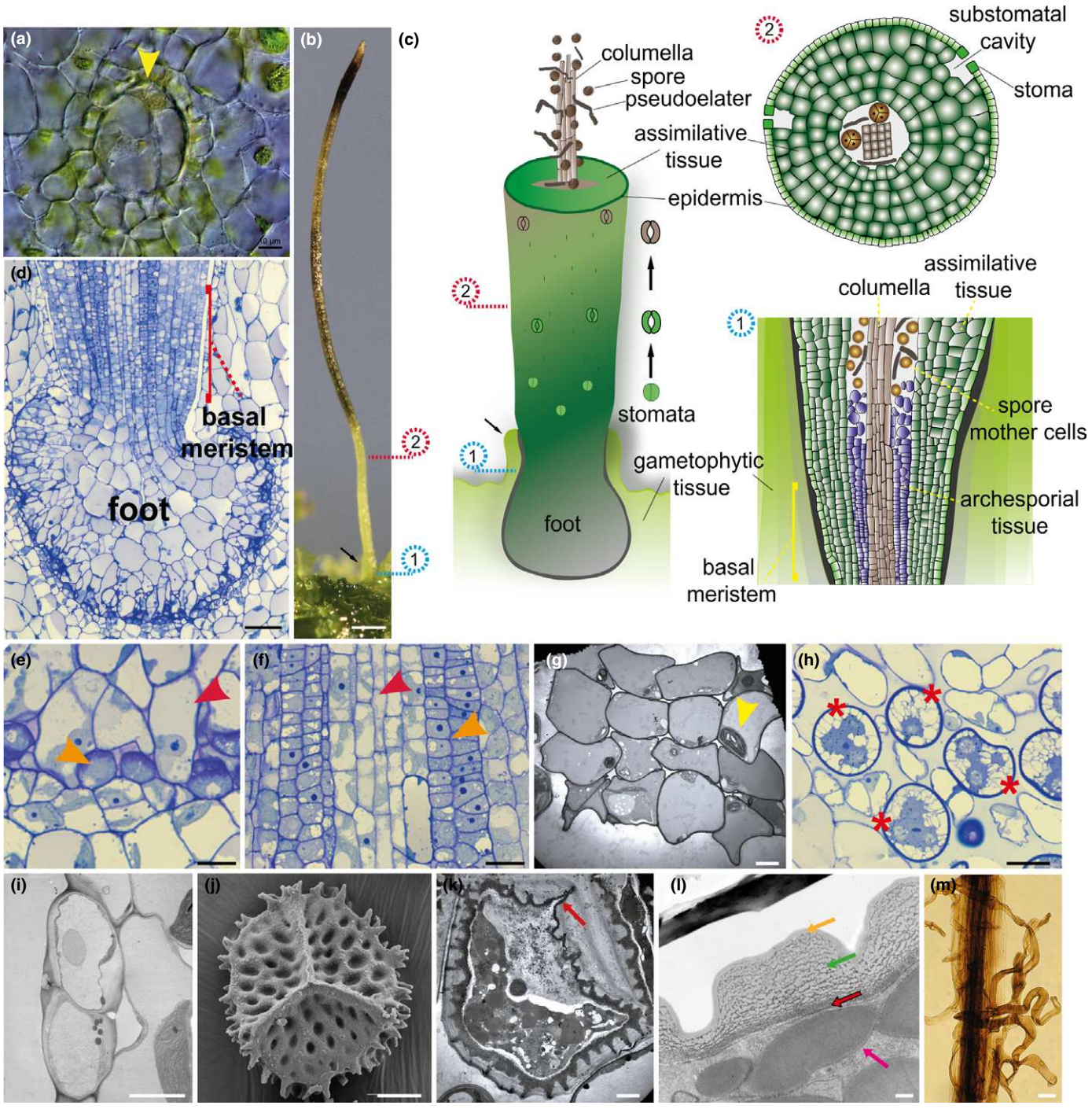

sporophyte of the liverwort *M. polymorpha* does not possess a well-defined meristematic region, and cell divisions occur throughout the developing tissue (Shimamura, 2016). In tracheophytes, the sporophyte grows from the SAM and root apical meristem, which are composed of one, two or numerous stem cells (Harrison, 2017). The mechanisms by which apical stem cell activity evolved in tracheophyte sporophytes remain elusive. It has been hypothesized that the tracheophyte SAM evolved from an embryonic apical meristem, similar to that present in extant mosses (Albert, 1999). Transcriptomic data suggest that tracheophyte meristems may have evolved independently in lycophytes, ferns and seed plants (Frank *et al.*, 2015). It has also been hypothesized that the hornwort basal meristem evolved into the tracheophyte SAM by displacement to the shoot apex (Ligrone *et al.*, 2012).

A series of studies have indicated that a small family of transcription factors called *KNOTTED1-LIKE HOMEOBOX* (*KNOX*) genes played a key role in the evolution of the land plant sporophyte (Hay & Tsiantis, 2010). *KNOX* genes are found in all green plant lineages, from chlorophytes to angiosperms. Insight into the role of *KNOX* genes in lineages that diverged before plants

Fig. 6 *Anthoceros agrestis* embryo and sporophyte. (a) Differential interference contrast image of embryo with first longitudinal division (yellow arrowhead). Bar, 10 μm. (b) Sporophyte. Spores mature progressively from the bottom to the top of the sporophyte. Involucre indicated with black arrow. Bar, 0.5 mm. (c) Schematic representation of sporophyte. The sporophyte has a foot, a basal meristem, the columella, a spore layer with pseudoelaters (for spore dispersal), a multicellular assimilative layer and stomata. Successive stages of stomata development are shown next to the sporophyte. Opening of the pore occurs near the base of the sporophyte then guard cells wall thickens, and guard cells collapse toward the upper part of the sporophyte, allowing dehydration and dehiscence into two valves. Involucre indicated with black arrow. Numbered circles indicate the relative position on the sporophyte that corresponds to the cartoons on the right of panel: 1, schematic representation of longitudinal section directly above the foot showing the basal meristem and differentiating sporogenous tissue; 2, schematic representation of transverse section showing, from centre to outside, columella, spores, pseudoelaters, assimilative tissue, epidermis and stomata with substomatal cavities. (d) Light microscopy (LM) longitudinal section of bulbous foot and basal meristem surrounded by the involucre. The placenta consists of elongated haustorial foot cells adjacent to small gametophyte cells. Bar, 50 μm. (e) Enlargement of placental cells in (d) showing smooth-walled haustorial cells (red arrowhead) intermixed with gametophyte cells (orange arrowhead) with conspicuous cell wall ingrowths (orange arrowhead). Bar, 10 μm. (f) LM longitudinal section of archesporial tissue (orange arrowhead) surrounding columella (red arrowhead) directly above the basal meristem. Bar, 20 μm. (g) Transmission electron microscopy (TEM) image of columella in cross-section showing 4 × 4 arrangement of the 16 living cells that contain dense cytosol and chloroplast (yellow arrowhead). Bar, 4.0 μm. (h) LM section showing spore mother cells (red asterisks) with three of four large starch-filled plastids in four poles and central nucleus preparing for meiosis. Bar, 20 μm. (i) TEM of dying and collapsing stoma (brown in (c)) showing thickened walls, inner and outer ledges of guard cells, and substomatal cavity. This section is on the polar end of the guard cells, away from the pore. Bar, 5 μm. (j) Scanning electron microscopy of a proximal surface of spore with a defined trilete mark. Bar, 10 μm. (k) TEM of spore in a tetrad still surrounded by the spore mother cell wall showing three-layered wall with ornamentation. The aperture on the proximal wall where spores in a tetrad meet each other has a thick intine and includes the trilete mark (red arrow). Bar, 4.0 μm. (l) TEM of mature spore wall composed of outer exine (orange arrow), thick inner exine with compressed globular sporopollenin (green arrow) and thin intine that is much like a primary cell wall (red arrow). Protein bodies fill the spore (pink arrow). Bar, 0.5 μm. (m) LM of dissected columella with elongated multicellular pseudoelaters attached. Bars, 25 μm.

colonized the land was provided by a study in the chlorophyte alga *Chlamydomonas reinhardtii* (Lee *et al.*, 2008). *C. reinhardtii* has two types of gametes, plus and minus, that express the KNOX protein GAMETE SPECIFIC MINUS 1 (GSM1) and the BELL protein GAMETE SPECIFIC PLUS 1 (GSP1), respectively. GSM1 and GSP1 proteins accumulate in the gametes, physically interact with each other upon gametic fusion and translocate from the cytosol to the nucleus to initiate zygote development.

KNOX genes have diversified into two subfamilies, class 1 and class 2 (Fig. 5). The duplication leading to class 1 and class 2 *KNOX* genes occurred within the ancestor of land plants and charophytes given that homologues for both classes have been identified in the charophytes *Spirogyra pratensis* (Frangedakis *et al.*, 2017) and *Klebsormidium nitens* (Hori *et al.*, 2014).

In *P. patens* class 1 *KNOX* genes acquired functions to control meristematic activity in the sporophyte (Sakakibara *et al.*, 2008; Coudert *et al.*, 2019) and class 2 *KNOX* genes evolved to maintain the diploid state through suppression of the gametophytic development programme (Sakakibara *et al.*, 2013). Similar to chlorophytes, land plant KNOX proteins function via the formation of heterodimers with BELL proteins. One of the four *BELL* genes in *P. patens*, *PpBELL1*, is necessary and sufficient for sporophyte development (Horst *et al.*, 2016). In *M. polymorpha* a class 1 KNOX protein is expressed in the egg and is necessary for the formation of the zygote via interaction with two paternally inherited BELL proteins (Mp*BELL3* and/or Mp*BELL4*) (Dierschke *et al.*, 2020), a function similar to the KNOX function in *C. reinhardtii*. The class 1 *KNOX*, another *MpBELL1* and class 2 *KNOX* genes, are also upregulated in the developing sporophytes of *M. polymorpha*, suggesting a role in sporophyte development (Frank & Scanlon, 2015; Flores-Sandoval *et al.*, 2018; Hisanaga *et al.*, 2020). Collectively, these observations indicate that the ancestral mechanism to initiate zygote development in *C. reinhardtii* was retained in *M. polymorpha* but also diversified to control sporophyte development in both *M. polymorpha* similar to *P. patens*. The function of *KNOX* genes further diversified during the evolution of tracheophytes to control shoot meristem establishment and maintenance as indicated by studies in the lycophyte *Selaginella kraussiana* and *A. thaliana* (Harrison *et al.*, 2005). Hornworts have only a single *KNOX* gene that belongs to the class 2 subfamily and a single *BELL* gene (Fig. 5). The presence of a single *KNOX* gene in the hornwort *A. agrestis* is an intriguing finding given that other bryophytes and charophytes carry both class 1 and 2 *KNOX* genes. A possible scenario is that the absence of class 1 *KNOX* genes in *A. agrestis* represents a secondary loss within hornworts, or at least within the genus *Anthoceros*. The function of class 2 *KNOX* genes in *A. agrestis* is unknown and may be key to understanding how the function of class 1 and 2 genes has diversified during land plant evolution.

5. Stomata development

Most hornworts have stomata on their sporophytes (Figs 2k,n, 6c). Recent studies suggest that stomata in hornworts are involved in sporophyte dehydration and spore dispersal (Renzaglia *et al.*, 2017; Pressel *et al.*, 2018). Stomata develop at the base of the sporophyte and initially consist of two guard cells covering a liquid-filled intercellular space (ICS) (Duckett & Pressel, 2018). Opening of the pore occurs near the base of the sporophyte before the guard cell wall thickens, which allows the liquid inside the ICS to evaporate, favouring the dehydration and dehiscence of the sporophyte (Fig. 6c,i). There is still an open debate on the different functions of stomata between tracheophytes and bryophytes. Tracheophytes have gas-filled ICSs, surrounded by guard cells which open and close in response to environmental cues, preventing water loss and optimizing CO_2 assimilation. By contrast, stomata of hornworts remain open after the pore is formed and they die and collapse before spore maturation (Merced & Renzaglia, 2017; Renzaglia *et al.*, 2017). It is hypothesized that this allows for the evaporation of the liquid inside the ICSs and to promote spore maturation and

dispersal. Hornwort stomata lack physiological responses to exogenous signals such as ABA, water availability and CO_2 (Pressel *et al.*, 2018). The small changes in the size of the aperture are probably the result of desiccation and not active closing of the pore. The different composition of guard cell walls in hornworts compared with *A. thaliana* supports the inability of hornwort stomata to regulate opening and closing of the pore (Merced & Renzaglia, 2019).

Stomatal development is regulated by a set of genes in *A. thaliana* (Chater *et al.*, 2016, 2017), including the *bHLH* transcription factors *SPCH*, *MUTE* and *FAMA* (*SMF*), ICE/SCREAM (*SCRM*), the signal peptide *EPIDERMAL PATTERNING FACTOR* (*EPF*), and its receptors *ERECTA* and *TOO MANY MOUTHS* (*TMM*) (Chater *et al.*, 2016; Lee & Bergmann, 2019). The origin of stomata (single or multiple) and the evolution of the developmental mechanism/functionality of stomata across land plants remain a topic of debate (Chater *et al.*, 2017; Renzaglia *et al.*, 2020). Recently, it was hypothesized that the common ancestor of embryophytes possessed the core genetic toolkit for stomata development, which were then lost or reduced during the evolution of bryophytes (Harris *et al.*, 2020). A gene encoding a protein similar to *SPCH*/*MUTE*/*FAMA*/*SMF* was present in the common ancestor of embryophytes. A duplication event led to its divergence into a *SPCH*/*MUTE* and a *FAMA*/*SMF* clade. The *FAMA*/*SMF* clade further diversified into a *FAMA* and an *SMF* clade before the divergence of tracheophytes and bryophytes. *SMF* was lost in most tracheophytes whereas *FAMA* and *SPCH*/*MUTE* were lost in all bryophytes (Harris *et al.*, 2020). *ERECTA*, *SCRM*, *EPF* and *TMM* homologues were also present in the common ancestor of embryophytes Harris *et al.*, 2020). In line with this hypothesis, orthologues of *SMF*, *SCRM*, *ERECTA*, *EPF* and *TMM* are present in *A. agrestis* (Fig. 5). *SMF*, *SCRM*, *TMM* and *EPF* are expressed in the sporophyte, suggesting that they may have similar roles in stomata development (Li *et al.*, 2020). Genetic studies in *A. agrestis* will help to elucidate the evolution of stomata in hornworts and across land plants.

V. The hornwort chloroplast

1. Monoplastidy

Chloroplasts evolved from an endosymbiotic event between a eukaryotic host and a photosynthetic prokaryote, more than 1 billion years ago (Jensen & Leister, 2014). Unique amongst land plants with the exception of a small number of lycophyte species, all hornworts have one (or just a few) chloroplast(s) per cell (Fig. 7) (Vaughn *et al.*, 1992; de Vries & Gould, 2018; Liu *et al.*, 2020). All other land plants have several chloroplasts per vegetative cell. The increase in number of chloroplasts per cell and the subsequent reduction in their size increases the surface area to volume ratio of the chloroplast, which leads to an enhanced photosynthetic efficiency (Xiong *et al.*, 2017). Another hypothesis states that many small chloroplasts allow movement and rearrangement within the cell for more effective light acclimatization (Trojan & Gabrys, 1996; Königer *et al.*, 2008), and reduces the chance of damage to the photosystem II (PSII) complex under high-light conditions (Park *et al.*, 1996). If one organelle is damaged, a cell has many more chloroplasts as back-up. The evolution of multiple chloroplasts per cell (polyplastidity) is poorly understood. The complete loss of the peptidoglycan (PG) layer of the chloroplast might be linked to the switch from mono- to polyplastidy in land plants, but it cannot be the only driving factor because the PG layer is absent in rhodophytes (Grosche & Rensing, 2017), which are predominantly monoplastidic. Hornworts are therefore a key group in understanding the evolution of polyplastidy in land plants.

Unlike the evolution of the mechanism that led to polyplastidy, the molecular mechanisms of plastid division in land plants is well understood (Fig. 7b) (Okazaki *et al.*, 2010; Chen *et al.*, 2018). Cell division, both mitosis and meiosis, in hornworts involves plastid divisions that are closely linked to the nuclear division (Fig. 7d,e) (Brown & Lemmon, 1990, 1993). In meiosis, the large starch-filled plastids migrate to the four poles and form the focal points for the

Fig. 7 *Anthoceros agrestis* chloroplast. (a) Schematic representation of the *Chlamydomonas reinhardtii* carbon-concentrating mechanism (CCM) model. The carbonic anhydrase (CAH2) converts CO_2 into HCO_3^- (dicarboxylate (DIC)) in the periplasmic space. DIC is pumped across membranes via DIC transporters localized in the plasma membrane (low-CO_2 inducible 1 (LCI1) and high light activated 3 (HLA3)), the chloroplast envelope (low-CO_2 inducible A (LCIA)) and the thylakoid membrane (low-CO_2 inducible 11 (LCI11), Cre16.g662600 and Cre16.g663400). The carbonic anhydrase 3 (CAH3) in the thylakoid lumen converts HCO_3^- into CO_2. supplied to Rubisco. EPYC1 acts as glue between Rubisco units in the pyrenoid. The low-CO_2 inducible B and C (LCIB/C) proteins are thought to form a molecular 'ring' around the pyrenoid that acts as a barrier to CO_2 leakage transferring CO_2 back to the thylakoid via the DIC pumps. (b) Top left boxes, genes of prokaryotic origin (in blue) and genes of land plant origin (in green) involved in chloroplast division in *Arabidopsis thaliana*. Genes absent in *A. agrestis* genome are in grey. Top right and bottom: schematic representation of the key elements of chloroplast division machinery in *A. thaliana* (Chen *et al.*, 2018). FtsZ1 and FtsZ2 self-assemble and then recruit ARC6, PARC6, PDV1, PDV2 and DRP5B, forming a ring around the chloroplast that mediates its division. IE, inner envelope; OE, outer envelope. (c) Surface view of sporophyte showing chloroplasts. Bar, 100 μm. (d) Light microscopy (LM) section of spore mother cell with plastids (three out of four visible) at poles indicated with asterisks. Bar, 15 μm. (e) LM of spore mother cell stained with DAPI showing DNA in central nucleus and plastids (orange arrowhead). Bar, 15 μm. (f) Cells of young gametophyte tissue with a single chloroplast and central pyrenoid surrounded by starch grains. Bar, 10 μm. (g) Cells of mature gametophyte tissue with single chloroplasts that have several protrusions that are probably stromules (orange arrowhead). Bar, 50 μm. (h–k) Transmission electron microscopy of chloroplasts of *A. agrestis*. (h) Chloroplast in an assimilative cell of sporophyte near intercellular space, with pyrenoid (red arrowhead) traversed by thylakoids (orange arrowhead) and small grana (yellow arrowhead). Starch granules are indicated by yellow arrowhead and thylakoids enlarged in (i) at yellow arrowhead. Bar, 2.0 μm. (i) Details of thylakoids and grana showing absence of end membranes. Bar, 0.5 μm. (j, k) Sporophyte chloroplast in an assimilative cell near intercellular space traversed by channel thylakoids and grana stacks (yellow arrowhead). Starch grains are indicated by an orange arrowhead. Pyrenoid is not in this nonmedian section. Bar, 500 nm. (k) Higher magnification (bar, 0.5 μm) of region indicated in (j) showing channel thylakoids. Bar, 2.0 μm. (l) Confocal microscopy image of *A. agrestis* transgenic gametophyte. Green: green fluorescent protein localized in the plasma membrane expressed under the *CaMV* 35S promoter. Red: chlorophyll autofluorescence. Orange arrowhead indicates chloroplast protrusions likely to be stromules. Bar, 10 μm. (m) Confocal microscopy image of a germinating spore highlighting the wavy 3D structure of the chloroplast. Red, chlorophyll autofluorescence. Bar, 20 μm.

quadripolar spindle (Fig. 7e). Throughout the process, plastid DNA is visible and abundant (Fig. 7d). A series of genes are known to be involved in plastid division machinery in *A. thaliana*, including the *Filamentous Temperature Sensitive Z 1* (*FtsZ1*), *FtsZ2*, *Accumulation and Replication of Chloroplast 6* (*ARC6*), *Dynamin-related protein 5B* (*DRP5B*), *Septum site-determining protein MinC*, *E* and *D*, *Plastid Division protein 2* (*PDV2*), *Plastid Division protein 1* (*PDV1*), *Multiple Chloroplast Division site 1*, *Paralogue of ARC6* (*PARC6*) and *Accumulation and Replication of Chloroplast 3* (*ARC3*) (Fig.7b). The *A. agrestis* genome lacks homologues of *PARC6* and

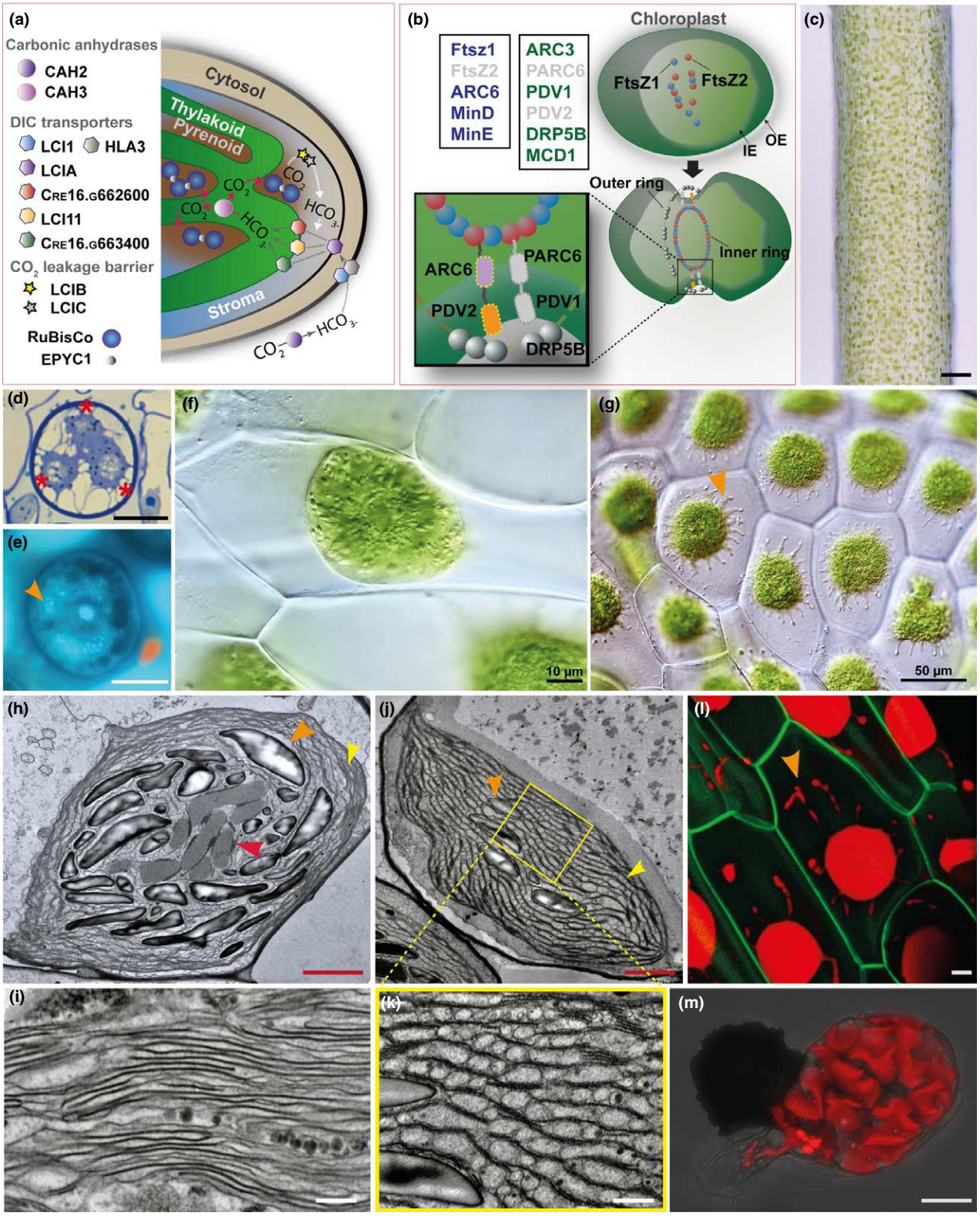

PDV1, consistent with the current understanding that they diversified after tracheophytes diverged, although *A. agrestis* also lacks an *FtsZ2* homologue (Fig. 7b) (Li *et al.*, 2020). *FtsZ2* knockout mutants in *P. patens* and *A. thaliana* (Martin *et al.*, 2009; Schmitz *et al.*, 2009) result in cells that contain a single chloroplast. This raises the question of whether the lack of *FtsZ2* in *A. agrestis* is related to its monoplastidy. *FtsZ2* is also absent in the streptophyte algae *Mesostigma viride*, *Chlorokybus atmophyticus* and *C. braunii* but not in *K. nitens* or Zygnematophyceae (Hori *et al.*, 2014; Nishiyama *et al.*, 2018; Cheng *et al.*, 2019; Wang *et al.*, 2020). It is possible that *FtsZ2* was present in the last common ancestor of land plants and streptophyte algae and then was lost several times or that *FtsZ2* had independent origins.

Cells of mature gametophyte tissue have tubular protrusions on the chloroplast, potentially stromules (Fig. 7g,l). Stromules have been found to be involved in various functions such as protein trafficking and effector-triggered immunity (Caplan *et al.*, 2015; Hanson & Hines, 2018).

2. The pyrenoid

Hornworts are the only land plant group that has pyrenoids (Figs 3d, 7a,h) (Villarreal & Renner, 2012), which are otherwise common in most unicellular algae (Meyer *et al.*, 2017). The pyrenoid is an unbound proteinaceous specialized compartment within the chloroplast that is mainly composed of the enzyme Rubisco (Meyer *et al.*, 2017).

Most of our current understanding about pyrenoids is based on studies in the alga *C. reinhardtii*. In aquatic environments a carbon-concentrating mechanism (CCM) is necessary for Rubisco to function efficiently because CO_2 diffuses 10 000 times slower in water than in air (Machingura & Moroney, 2018). The CCM in *C. reinhardtii* (Fig. 7a) involves a carbonic anhydrase (CAH2) in the periplasmic space that converts CO_2 to bicarbonate (HCO_3^-). Then transport proteins, both on the cell (low-CO_2 inducible 1 (LCI1) and high light activated 3 (HLA3)), chloroplast (low-CO_2 inducible A (LCIA), Cre16.g662600 and Cre16.g663400) and thylakoid (low-CO_2 inducible 1 (LCI11)) membranes, pump bicarbonate (HCO_3^-) from the environment, into the cell and into the chloroplast thylakoids (Wang *et al.*, 2015). In the chloroplast thylakoids, CAH3 converts HCO_3^- to CO_2 (Aspatwar *et al.*, 2018) resulting in an up to 50-fold increase of CO_2 concentration in the pyrenoids and improving the photosynthetic efficiency of Rubisco. In the pyrenoid of *C. reinhardtii*, Rubisco is scaffolded by the *Essential Pyrenoid Component 1* (*EPYC1*) protein (Mackinder *et al.*, 2016), which functions as a 'glue'. The remaining proteins that compose the algal pyrenoid include Rubisco-interacting proteins, photosystem I (PSI) assembly factor candidates and inorganic carbon flux components (Mackinder *et al.*, 2017).

One main difference between the hornwort and algal chloroplast is the presence of grana (Fig. 7h–k), stacked thylakoids that compartmentalize chloroplast space, are enriched in PSII and allow more efficient light capturing (Wilsenach, 1963; Burr, 1970; Renzaglia *et al.*, 2009). Grana in hornworts lack the highly curved end membranes that are common in the chloroplast of other land plants, suggesting biochemical differences (Fig. 7i) (Vaughn *et al.*, 1992). Another unique feature of the hornwort chloroplast is the presence of thylakoids that connect adjacent grana, at a right angle to the long axis of the granum, called channel thylakoids. Channel thylakoids function in separating space within the chloroplast stroma (Fig. 7k) and are enriched in PSI. In the majority of hornworts, pyrenoids have multiple subunits traversed by thylakoids and may be encircled by an outer starch sheath (Fig. 7h). In *A. agrestis*, the pyrenoid in vegetative cells consists of lens-shaped electron-dense units delineated by thylakoids and small grana (Fig. 7h). On an anatomical level there is considerable variability in chloroplasts across hornworts. A notable example is the epiphytic *Dendroceros* that possesses star-shaped plastids with a large central pyrenoid containing globular units. Pyrenoidless species include *Paraphymatoceros*, *Megaceros* and some *Nothoceros* (up to 14 plastids per cell). In *Leiosporoceros*, the sister taxon to the remaining hornworts, the pyrenoidless chloroplasts have a central aggregation of massive grana, which may represent the ancestral condition in the clade.

Hornwort pyrenoids evolved independently from streptophyte algae pyrenoids (Villarreal & Renner, 2012). Genomic and transcriptomic data show that some *C. reinhardtii* CCM components, such as the *CAH3*, the *LCI11* and the *low-CO_2 inducible B* (*LCIB*) genes (Fig. 7a), have putative homologues in hornworts (Li *et al.*, 2020). In *C. reinhardtii*, LCIB proteins localize around pyrenoids and are hypothesized to prevent CO_2 leakage from the pyrenoids (Yamano *et al.*, 2010; Jin *et al.*, 2016) (Fig. 7a). However, several other *C. reinhardtii* pyrenoid-related genes, such as *EPYC1*, are absent in the genome of *A. agrestis*. To what extent hornwort pyrenoids share more common traits with streptophyte algae pyrenoids remains to be explored.

3. RNA editing

Hornworts have one of the highest levels of chloroplast RNA editing amongst all land plants studied to date (Kugita *et al.*, 2003). RNA editing is a form of nucleotide sequence alteration that occurs at the transcriptional level in the chloroplast (Small *et al.*, 2019). RNA editing converts cytidines (C) to uridines (U) (C-to-U, called canonical RNA editing) or uridines to cytidines (U-to-C, called reverse editing) in mRNAs before their translation. As a consequence, a sense codon can be converted into a more evolutionarily conserved one or a start/stop codon to a sense codon (Tillich *et al.*, 2006). Organelles in *A. agrestis* feature high amounts of RNA editing with altogether more than 1100 sites of C-to-U and 1300 sites of U-to-C editing (Gerke *et al.*, 2019).

The nuclear genome also reveals over 1400 genes for PPR proteins (Li *et al.*, 2020). PPR proteins are a group of RNA-binding proteins which play critical roles in post-transcriptional gene regulation in plant chloroplasts (Barkan & Small, 2014). Preliminary data suggest that the few land plant lineages capable of reverse editing have evolved special types of PPR proteins, providing strong candidates for future studies (Gerke *et al.*, 2019; Gutmann *et al.*, 2020). *A. agrestis* provides an exceptional system to study the poorly known mechanisms and the evolution of reverse editing in land plants.

VI. Symbiosis

Hornworts establish two types of symbiotic relationships: with cyanobacteria and with arbuscular mycorrhizal fungi (AMF) (Fig. 8).

1. Cyanobacteria symbiosis

Cyanobacteria are prokaryotes possessing the ability to perform photosynthesis and to fix atmospheric nitrogen, thus providing the host with usable nitrogen (Adams & Duggan, 2008). The earliest evidence of cyanobacteria growing within the tissue of a land plant comes from *Aglaophyton major* fossils (Krings *et al.*, 2009). This suggests that land plant–cyanobacteria associations are probably at least 400 milion years old. Symbiosis of land plants with nitrogen-fixing cyanobacteria is uncommon, but in hornworts endophytic associations are ubiquitous (Fig. 8a–d,h) (Renzaglia *et al.*, 2009). The other bryophyte group that has an endophytic symbiotic relationship with cyanobacteria are liverworts (Adams, 2002), but

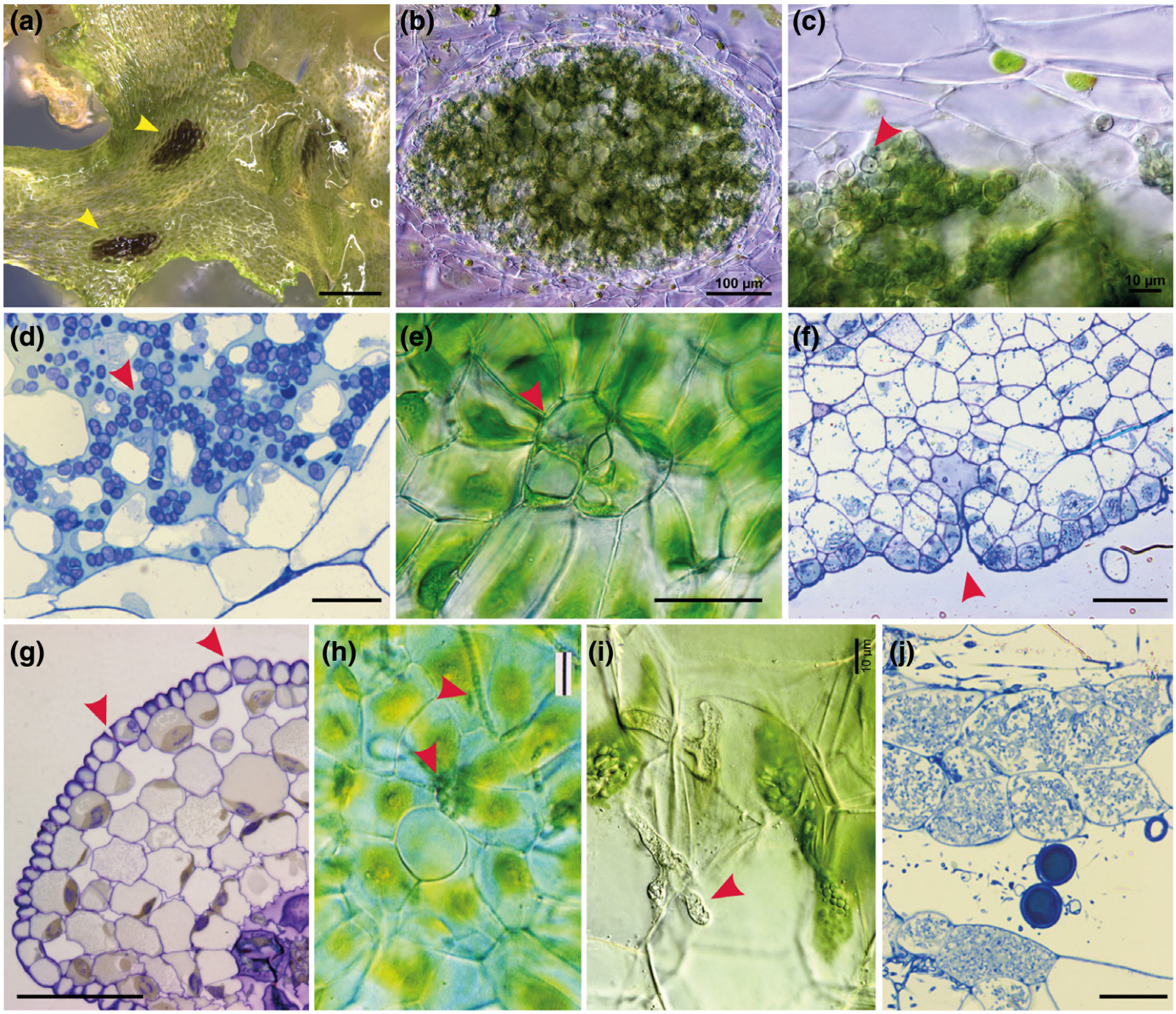

Fig. 8 Hornwort symbiotic relationships. (a) Surface view of *Anthoceros puncatus* thallus colonized by cyanobacteria (yellow arrowheads). Bar, 450 µm. (b, c) Hand sections of *A. punctatus* thallus showing ellipsoidal cavities colonized by cyanobacteria. In (c) cyanobacteria indicated with red arrowhead. Bars, 100 µm (b), 10 µm (c). (d) Light microscopy (LM) section of *Nostoc* colony showing algal cells (red arrowhead) with intermingling gametophyte cells in *A. agrestis*. Bar, 10 µm. (e) LM surface view of ventral mucilage cleft (red arrowhead). Bar, 15 µm. (f) Longitudinal section of a mucilage cleft (red arrowhead) leading to small intercellular space near apical notch of *A. agrestis*. Bar, 50 µm. (g) LM transverse section of sporophyte showing guard cells in epidermis that lead to substomatal cavities (red arrowhead). Guard cells are larger than epidermal cells and have differentially thickened cell walls with inner and outer ledges and are different from the mucilage cleft cells in (f) that have evenly thickened walls. Bar, 50 µm. (h) LM showing surface view of a mucilage cleft and attracted cyanobacteria (red arrowhead) just entering the cleft in *Phaeoceros carolinianus*. Bar, 20 µm. (i, j) Hornwort symbiotic relationship with arbuscular mycorrhizal fungi. Hand section LM of *P. carolinianus* thallus cells with fungal hyphae (red arrowhead). Bar, 10 µm. (j) LM section of gametophyte cells containing vesicles (circles) and arbuscules (masses of hyphae in cells). Bar, 20 µm.

this is rare as it occurs in only two closely related genera: *Blasia* and *Cavicularia* (Meeks, 1998). Cyanobacterial endosymbiosis is also found in the water fern *Azolla* (Whitton, 1993), cycads (Lindblad & Bergman, 2018) and *Gunnera* (an angiosperm) (Bergman *et al.*, 1992).

Cyanobacteria that establish symbiotic relationships with plants are primarily members of the polyphyletic genus *Nostoc* (Dodds *et al.*, 1995; Rai *et al.*, 2002). Amongst all the land plant associations with cyanobacteria, most of the research has been done on hornworts, using *A. punctatus* (Fig. 8a–c) and the cyanobacterium *Nostoc punctiforme* as the study system (Meeks, 2003). Recent transcriptomic data from both *A. punctatus* and *A. agrestis* growing with or without *N. punctiforme* identified 40 candidate genes that may play a role in the symbiotic relationship (Li *et al.*, 2020). Those genes include receptor kinases, transcription factors and transporters.

2. Mucilage cleft

An innovation of the hornwort gametophyte was mucilage clefts (Figs 2e, 8e,f,h). Mucilage clefts are usually two-celled epidermal structures that provide a pore for *Nostoc* cyanobacteria symbionts to enter and lead to a small mucilage-filled cavity (Renzaglia *et al.*, 2009) (Fig. 8f). Superficially they bear a resemblance to sporophyte stomata in that there are typically two cells surrounding a pore (compare Figs 2n and 8e). However, unlike guard cells, the cells surrounding the opening in mucilage clefts are not specialized and lack cell wall ledges and differential thickenings (Fig. 8f,g). Mucilage clefts are ephemeral and once *Nostoc* cyanobacteria enter the cleft, the epidermal cells increase in size and number and close the opening to the outside (Renzaglia, 1978). The *Nostoc* and gametophyte cells proliferate in synchrony, producing an ellipsoidal colony with intermingling algal and hornwort cells (Fig. 8a–d). The presence of pores in both generations of *A. agrestis* resembles observations made on the fossil plant *A. major* (Krings *et al.*, 2009).

An *EPF-like* gene belonging to the *EPFL4-6* clade was found in the *A. agrestis* genome, which is specifically expressed in gametophytes (Li *et al.*, 2020). This raises the possibility that the *A. agrestis EPF-like* gene is involved in mucilage cleft formation, possibly controlling separation between cells to make a pore and perhaps the production of a small ICS comparable to the substomatal cavity.

3. Arbuscular mycorrhizal fungi

The symbiotic relationship with AMF (Fig. 8i,j) is a key innovation underlying plant colonization of terrestrial environments. The fungal endophytes of *A. agrestis* include Mucoromycotina and/or Glomeromycota (Desirò *et al.*, 2013; Villarreal *et al.*, 2015). AMF are present in the majority of extant land plants. Recent studies have identified a series of genes in the angiosperms that regulate the establishment and maintenance of AMF symbiosis. All the key angiosperm AMF symbiosis genes have orthologues in the *A. agrestis* genome (Li *et al.*, 2020).

VII. Photoreceptors

Hornworts harbour a unique chimeric photoreceptor called neochrome, that is composed of a red/far-red-sensing module from the phytochrome and a blue-sensing phototropin (Li *et al.*, 2014, 2015a,b). Neochrome was initially discovered in ferns (Nozue *et al.*, 1998) and was considered a key innovation enabling ferns to diversify in the low-light angiosperm canopies (Kawai *et al.*, 2003; Schneider *et al.*, 2004). Through transcriptome- and genome-mining, Li *et al* (2014) found that among land plants, neochrome is restricted to ferns and hornworts, and they demonstrated that fern neochrome sequences were phylogenetically nested within those of hornworts. Such a nested relationship suggests that the fern neochrome was horizontally acquired from hornworts. Interestingly, hornwort phototropin lacks introns, similar to neochrome but unlike all other phototropin genes that typically have > 20 introns (Li *et al.*, 2014, 2015b). This implies that neochrome probably originated in hornworts, possibly through a retrotransposition event.

The function of neochrome in hornworts is unknown. In ferns, neochrome integrates red/far-red and blue light to orchestrate phototropism and chloroplast relocation. However, no phototropic response has been recorded in hornworts, and because most cells contain only a single chloroplast that occupies a large portion of the cellular space, it is unclear how directional chloroplast movement is possible or even necessary. By contrast, hornwort chloroplasts can contract and expand in response to light intensity (Burr, 1969; Li *et al.*, 2014); whether this is mediated by neochrome awaits future studies.

VIII. Conclusions

The development of *A. agrestis* as a hornwort experimental system, the sequencing of its genome and the availability of genetic manipulation methods will greatly facilitate efforts towards a more comprehensive study of the mechanisms underpinning land plant evolution. It will also provide detailed understanding of hornwort biology.

Synthetic biological approaches (Liu & Neal Stewart, 2015; Benning & Sweetlove, 2016) can also be used to engineer hornwort traits in crops. Engineering pyrenoids, for example, into plants with agronomic value has the potential to increase carbon fixation and therefore increase crop yield (Li *et al.*, 2017). Similarly, the hornwort–cyanobacteria symbiosis may hold the key to engineering crops with enhanced yield without increasing the amount of synthetic fertilizer. It is envisaged that detailed insights into the biology of hornworts have great potential to contribute to various fields of synthetic biology.

Acknowledgements

We acknowledge: National Science Foundation (NSF) grants DEB1831428 and IOS1923011 to FWL. Swiss National Science Foundation grants 160004, 131726 and 184826 to PS; NSF grant DUE-1758497 and NIH 5R25GM107760-07 to KSR; funding from the Georges and Antoine Claraz Foundation to PS and MW;

funding from The Forschungskredit and the University Research Priority Program 'Evolution in Action' of the University of Zurich to MW and PS; and Japan Society for the Promotion of Science (JSPS) grant nos. KAKENHI 26650143 and 18K06367 to KS; and The Deutsche Forschungsgemeinschaft (DFG – German Research Foundation) under the Priority Programme 'MAdLand – Molecular Adaptation to Land: Plant Evolution to Change' (SPP 2237, 440370263). [Correction added after online publication 15 September 2020: the Acknowledgements section has been updated.]

ORCID

Eftychios Frangedakis https://orcid.org/0000-0002-3483-8464
Fay-Wei Li https://orcid.org/0000-0002-0076-0152
Karen S. Renzaglia https://orcid.org/0000-0002-1406-2646
Keiko Sakakibara https://orcid.org/0000-0003-4420-9351
Masaki Shimamura https://orcid.org/0000-0002-5665-5116
Péter Szövényi https://orcid.org/0000-0002-0324-4639
Marta Tomaselli https://orcid.org/0000-0003-3470-2820
Juan Carlos Villarreal https://orcid.org/0000-0002-0770-1446
Manuel Waller https://orcid.org/0000-0002-6060-0740

References

Adams DG. 2002. Cyanobacteria in symbiosis with hornworts and liverworts. In: Rai AN, Bergman B, Rasmussen U, eds. *Cyanobacteria in symbiosis*. Dordrecht, the Netherlands: Springer, 117–135.

Adams DG, Duggan PS. 2008. Cyanobacteria–bryophyte symbioses. *Journal of Experimental Botany* **59**: 1047–1058.

Albert VA. 1999. Shoot apical meristems and floral patterning: an evolutionary perspective. *Trends in Plant Science* **4**: 84–86.

Aspatwar A, Susanna H, Seppo P. 2018. An update on the metabolic roles of carbonic anhydrases in the model alga *Chlamydomonas reinhardtii*. *Metabolites* **8**: 22–38.

Barkan A, Small I. 2014. Pentatricopeptide repeat proteins in plants. *Annual Review of Plant Biology* **65**: 415–442.

Barton MK. 2010. Twenty years on: the inner workings of the shoot apical meristem, a developmental dynamo. *Developmental Biology* **341**: 95–113.

Bennett TA, Liu MM, Aoyama T, Bierfreund NM, Braun M, Coudert Y, Dennis RJ, O'Connor D, Wang XY, White CD *et al.* 2014. Plasma membrane-targeted PIN proteins drive shoot development in a moss. *Current Biology* **24**: 2776–2785.

Benning C, Sweetlove L. 2016. Synthetic biology for basic and applied plant research. *The Plant Journal* **87**: 3–4.

Bergman B, Johansson C, Soderback E. 1992. The *Nostoc–Gunnera* symbiosis. *New Phytologist* **122**: 379–400.

Bernhardt C, Lee MM, Gonzalez A, Zhang F, Lloyd A, Schiefelbein J. The bHLH genes GLABRA3 (GL3) and ENHANCER OF GLABRA3 (EGL3) specify epidermal cell fate in the Arabidopsis root. *Development* **130**: 6431–6439.

Bowman JL, Kohchi T, Yamato KT, Jenkins J, Shu S, Ishizaki K, Yamaoka S, Nishihama R, Nakamura Y, Berger F *et al.* 2017. Insights into land plant evolution garnered from the *Marchantia polymorpha* genome. *Cell* **171**: 287–299.

Bowman JL, Sakakibara K, Furumizu C, Dierschke T. 2016. Evolution in the cycles of life. *Annual Review of Genetics* **50**: 133–154.

Breuninger H, Rikirsch E, Hermann M, Ueda M, Laux T. 2008. Differential expression of *WOX* genes mediates apical–basal axis formation in the *Arabidopsis* embryo. *Developmental Cell* **14**: 867–876.

Brown RC, Lemmon BE. 1990. Monoplastidic cell division in lower land plants. *American Journal of Botany* **77**: 559–571.

Brown RC, Lemmon BE. 1993. Diversity of cell division in simple land plants holds clues to evolution of the mitotic and cytokinetic apparatus in higher plants. *Memoirs of the Torrey Botanical Club* **25**: 45–62.

Burr FA. 1969. Chloroplast structure and division in *Megaceros* species. *Bryologist* **72**: 200–209.

Burr FA. 1970. Phylogenetic transitions in the chloroplasts of the Anthocerotales. I. The number and ultrastructure of the mature plastids. *American Journal of Botany* **57**: 97–110.

Campbell DH. 1918. *The structure and development of mosses and ferns (archegoniate), 3rd edn.* New York, NY, USA: Macmillan.

Caplan JL, Kumar AS, Park E, Padmanabhan MS, Hoban K, Modla S, Czymmek K, Dinesh-Kumar SP. 2015. Chloroplast stromules function during innate immunity. *Developmental Cell* **34**: 45–57.

Cargill DC, Christine Cargill D, Renzaglia KS, Villarreal JC, Joel Duff R. 2005. Generic concepts within hornworts: historical review, contemporary insights and future directions. *Australian Systematic Botany* **18**: 7.

Catarino B, Hetherington AJ, Emms DM, Kelly S, Dolan L. 2016. The stepwise increase in the number of transcription factor families in the precambrian predated the diversification of plants on land. *Molecular Biology and Evolution* **33**: 2815–2819.

Chater CCC, Caine RS, Fleming AJ, Gray JE. 2017. Origins and evolution of stomatal development. *Plant Physiology* **174**: 624–638.

Chater CC, Caine RS, Tomek M, Wallace S, Kamisugi Y, Cuming AC, Lang D, MacAlister CA, Casson S, Bergmann DC *et al.* 2016. Origin and function of stomata in the moss *Physcomitrella patens*. *Nature Plants* **2**: 16179.

Chen C, MacCready JS, Ducat DC, Osteryoung KW. 2018. The molecular machinery of chloroplast division. *Plant Physiology* **176**: 138–151.

Cheng S, Xian W, Fu Y, Marin B, Keller J, Wu T, Sun W, Li X, Xu Y, Zhang Y *et al.* 2019. Genomes of subaerial Zygnematophyceae provide insights into land plant evolution. *Cell* **179**: 1057–1067.e14.

Coudert Y, Novák O, Harrison CJ. 2019. A KNOX-Cytokinin regulatory module predates the origin of indeterminate vascular plants. *Current Biology* **29**: 2743–2750.e5.

Dawes TN, Villarreal JCA, Szövényi P, Bisang I, DA LiFW Hauser, Quandt D, Cargill DC, Forrest LL. 2020. Molecular data shows a recent European origin of the model bryophyte *Anthoceros agrestis*. *Plant Systematics and Evolution* **306**: 49.

de Vries J, Gould SB. 2018. The monoplastidic bottleneck in algae and plant evolution. *Journal of Cell Science* **131**: jcs203414.

Delwiche CF, Cooper ED. 2015. The evolutionary origin of a terrestrial flora. *Current Biology* **25**: R899–R910.

Denis E, Kbiri N, Mary V, Claisse G, Conde E Silva N, Kreis M, Deveaux Y. 2017. *WOX14* promotes bioactive gibberellin synthesis and vascular cell differentiation in *Arabidopsis*. *The Plant Journal* **90**: 560–572.

Desirò A, Duckett JG, Pressel S, Villarreal JC, Bidartondo MI. 2013. Fungal symbioses in hornworts: a chequered history. *Proceedings. Biological Sciences/The Royal Society* **280**: 20130207.

Di Cristina M, Sessa G, Dolan L, Linstead P, Baima S, Ruberti I, Morelli G. 1996. The *Arabidopsis* Athb-10 (GLABRA2) is an HD-Zip protein required for regulation of root hair development. *The Plant Journal* **10**: 393–402.

Dierschke T, Flores-Sandoval E, Rast-Somssich MI, Althoff F, Zachgo S, Bowman JL. 2020. Gamete-specific expression of TALE class HD genes activates the diploid sporophyte program in *Marchantia polymorpha*. *bioRxiv*. doi: 10.1101/2020.04.06.027821.

Dodds WK, Gudder DA, Mollenhauer D. 1995. The ecology of *Nostoc*. *Journal of Phycology* **31**: 2–18.

Duckett JG, Pressel S. 2018. The evolution of the stomatal apparatus: intercellular spaces and sporophyte water relations in bryophytes-two ignored dimensions. *Philosophical Transactions of the Royal Society of London. Series B, Biological Sciences* **373**: 20160498.

Duff RJ, Villarreal JC, Cargill CD, Renzaglia KS. 2007. Progress and challenges toward developing a phylogeny and classification of the hornworts. *Bryologist* **110**: 214–243.

Flores-Sandoval E, Romani F, Bowman JL. 2018. Co-expression and transcriptome analysis of *Marchantia polymorpha* transcription factors supports class C ARFs as independent actors of an ancient auxin regulatory module. *Frontiers in Plant Science* **9**: 1345.

Frangedakis E, Saint-Marcoux D, Moody LA, Rabbinowitsch E, Langdale JA. 2017. Nonreciprocal complementation of *KNOX* gene function in land plants. *New Phytologist* **216**: 591–604.

Frank MH, Edwards MB, Schultz ER, McKain MR, Fei Z, Sørensen I, Rose JKC, Scanlon MJ. 2015. Dissecting the molecular signatures of apical cell-type shoot meristems from two ancient land plant lineages. *New Phytologist* **207**: 893–904.

Frank MH, Scanlon MJ. 2015. Transcriptomic evidence for the evolution of shoot meristem function in sporophyte-dominant land plants through concerted selection of ancestral gametophytic and sporophytic genetic programs. *Molecular Biology and Evolution* **32**: 3033.

Gerke P, Szövényi P, Neubauer A, Lenz H, Gutmann B, McDowell R, Small I, Schallenberg-Rüdinger M, Knoop V. 2019. Towards a plant model for enigmatic U-to-C RNA editing: the organelle genomes, transcriptomes, editomes and candidate RNA editing factors in the hornwort *Anthoceros agrestis*. *New Phytologist* **225**: 1974–1992.

Goad DM, Zhu C, Kellogg EA. 2017. Comprehensive identification and clustering of *CLV3/ESR*-related (*CLE*) genes in plants finds groups with potentially shared function. *New Phytologist* **216**: 605–616.

van der Graaff E, Laux T, Rensing SA. 2009. The WUS homeobox-containing (WOX) protein family. *Genome Biology* **10**: 248.

Grosche C, Rensing SA. 2017. Three rings for the evolution of plastid shape: a tale of land plant FtsZ. *Protoplasma* **254**: 1879–1885.

Gutmann B, Royan S, Schallenberg-Rüdinger M, Lenz H, Castleden IR, McDowell R, Vacher MA, Tonti-Filippini J, Bond CS, Knoop V *et al.* 2020. The expansion and diversification of pentatricopeptide repeat RNA-editing factors in plants. *Molecular Plant* **13**: 215–230.

Haecker A, Gross-Hardt R, Geiges B, Sarkar A, Breuninger H, Herrmann M, Laux T. 2004. Expression dynamics of *WOX* genes mark cell fate decisions during early embryonic patterning in Arabidopsis thaliana. *Development* **131**: 657–668.

Hanson MR, Hines KM. 2018. Stromules: probing formation and function. *Plant Physiology* **176**: 128–137.

Harholt J, Moestrup Ø, Ulvskov P. 2016. Why plants were terrestrial from the beginning. *Trends in Plant Science* **21**: 96–101.

Harris BJ, Harrison CJ, Hetherington AM, Williams TA. 2020. Phylogenomic evidence for the monophyly of bryophytes and the reductive evolution of stomata. *Current Biology* **30**: 2001–2012.e2.

Harrison CJ, Corley SB, Moylan EC, Alexander DL, Scotland RW, Langdale JA. 2005. Independent recruitment of a conserved developmental mechanism during leaf evolution. *Nature* **434**: 509–514.

Harrison JC. 2017. Development and genetics in the evolution of land plant body plans. *Philosophical Transactions of the Royal Society of London. Series B, Biological Sciences* **372**: 20150490.

Hay A, Tsiantis M. 2010. *KNOX* genes: versatile regulators of plant development and diversity. *Development* **137**: 3153–3165.

Hirakawa Y, Bowman JL. 2015. A role of TDIF peptide signaling in vascular cell differentiation is conserved among euphyllophytes. *Frontiers in Plant Science* **6**: 1048.

Hirakawa Y, Kondo Y, Fukuda H. 2010. TDIF peptide signaling regulates vascular stem cell proliferation via the *WOX4* homeobox gene in *Arabidopsis*. *The Plant Cell* **22**: 2618–2629.

Hirakawa Y, Sawa S. 2019. Diverse function of plant peptide hormones in local signalling and development. *Current Opinion in Plant Biology* **51**: 81–87.

Hirakawa Y, Shinohara H, Kondo Y, Inoue A, Nakanomyo I, Ogawa M, Sawa S, Ohashi-Ito K, Matsubayashi Y, Fukuda H. 2008. Non-cell-autonomous control of vascular stem cell fate by a CLE peptide/receptor system. *Proceedings of the National Academy of Sciences USA* **105**: 15208–15213.

Hirakawa Y, Uchida N, Yamaguchi YL, Tabata R, Ishida S, Ishizaki K, Nishihama R, Kohchi T, Sawa S, Bowman JL. 2019. Control of proliferation in the haploid meristem by CLE peptide signaling in *Marchantia polymorpha*. *PLoS Genetics* **15**: e1007997.

Hisanaga T, Fujimoto S, Cui Y, Sato K, Sano R, Yamaoka S, Kohchi T, Berger F, Nakajima K. 2020. Deep evolutionary origin of gamete-directed zygote activation by KNOX/BELL transcription factors in green plants. *bioRxiv*. doi: 10.1101/2020.04.08.031930.

Honkanen S, Thamm A, Arteaga-Vazquez MA, Dolan L. 2018. Negative regulation of conserved RSL class I bHLH transcription factors evolved independently among land plants. *eLife* **7**: e38529.

Hori K, Maruyama F, Fujisawa T, Togashi T, Yamamoto N, Seo M, Sato S, Yamada T, Mori H, Tajima N *et al.* 2014. *Klebsormidium flaccidum* genome reveals primary factors for plant terrestrial adaptation. *Nature Communications* **5**: 3978.

Horst NA, Katz A, Pereman I, Decker EL, Ohad N, Reski R. 2016. A single homeobox gene triggers phase transition, embryogenesis and asexual reproduction. *Nature Plants* **2**: 15209.

Jensen PE, Leister D. 2014. Chloroplast evolution, structure and functions. *F1000Prime Reports* **6**: 40.

Jin S, Sun J, Wunder T, Tang D, Cousins AB, Sze SK, Mueller-Cajar O, Gao Y-G. 2016. Structural insights into the LCIB protein family reveals a new group of β-carbonic anhydrases. *Proceedings of the National Academy of Sciences, USA* **113**: 14716–14721.

Johnson GP, Renzaglia KS. 2009. Evaluating the diversity of pteridophyte embryology in the light of recent phylogenetic analyses leads to new inferences on character evolution. *Plant Systematics and Evolution* **283**: 149–164.

Jones VAS, Dolan L. 2012. The evolution of root hairs and rhizoids. *Annals of Botany* **110**: 205–212.

Kamiya N, Nagasaki H, Morikami A, Sato Y, Matsuoka M. 2003. Isolation and characterization of a rice *WUSCHEL*-type homeobox gene that is specifically expressed in the central cells of a quiescent center in the root apical meristem. *The Plant Journal* **35**: 429–441.

Kawai H, Kanegae TT, Christensen S, Kiyosue T, Sato Y, Imaizumi T, Kadota A, Wada MM. 2003. Responses of ferns to red light are mediated by an unconventional photoreceptor. *Nature* **421**: 287–290.

Kenrick P. 2018. Changing expressions: a hypothesis for the origin of the vascular plant life cycle. *Philosophical Transactions of the Royal Society of London. Series B: Biological Sciences* **373**: 20170149.

Kim H-J, Wu C-Y, Yu H-M, Sheen J, Lee H. 2017. Dual CLAVATA3 peptides in *Arabidopsis* shoot stem cell signaling. *Journal of Plant Biology* **60**: 506–512.

Kofuji R, Hasebe M. 2014. Eight types of stem cells in the life cycle of the moss *Physcomitrella patens*. *Current Opinion in Plant Biology* **17**: 13–21.

Königer M, Delamaide JA, Marlow ED, Harris GC. 2008. *Arabidopsis thaliana* leaves with altered chloroplast numbers and chloroplast movement exhibit impaired adjustments to both low and high light. *Journal of Experimental Botany* **59**: 2285–2297.

Krings M, Hass H, Kerp H, Taylor TN, Agerer R, Dotzler N. 2009. Endophytic cyanobacteria in a 400-million-yr-old land plant: a scenario for the origin of a symbiosis? *Review of Palaeobotany and Palynology* **153**: 62–69.

Kugita M, Yamamoto Y, Fujikawa T, Matsumoto T, Yoshinaga K. 2003. RNA editing in hornwort chloroplasts makes more than half the genes functional. *Nucleic Acids Research* **31**: 2417–2423.

Langdale JA. 2008. Evolution of developmental mechanisms in plants. *Current Opinion in Genetics & Development* **18**: 368–373.

Laux T, Mayer KF, Berger J, Jürgens G. 1996. The WUSCHEL gene is required for shoot and floral meristem integrity in *Arabidopsis*. *Development* **122**: 87–96.

Lee JH, Lin H, Joo S, Goodenough U. 2008. Early sexual origins of homeoprotein heterodimerization and evolution of the plant KNOX/BELL family. *Cell* **133**: 829–840.

Lee LR, Bergmann DC. 2019. The plant stomatal lineage at a glance. *Journal of Cell Science* **132**: jcs228551.

Leebens-Mack JH, Barker MS, Carpenter EJ, Deyholos MK, Gitzendanner MA, *et al.* 2019. One thousand plant transcriptomes and the phylogenomics of green plants. *Nature* **574**: 679–685.

Li F-W, Brouwer P, Carretero-Paulet L, Cheng S, de Vries J, Delaux PM, Eily A, Koppers N, Kuo LY, Li Z *et al.* 2018. Fern genomes elucidate land plant evolution and cyanobacterial symbioses. *Nature Plants* **4**: 460–472.

Li F-W, Melkonian M, Rothfels CJ, Villarreal JC, Stevenson DW, Graham SW, Wong GK-S, Pryer KM, Mathews S. 2015a. Phytochrome diversity in green plants and the origin of canonical plant phytochromes. *Nature Communications* **6**: 1–12.

Li F-W, Nishiyama T, Waller M, Frangedakis E, Keller J, Li Z, Fernandez-Pozo N, Barker MS, Bennett T, Blázquez MA *et al.* 2020. Anthoceros genomes illuminate the origin of land plants and the unique biology of hornworts. *Nature Plants* **6**: 259–272.

Li F-W, Rothfels CJ, Melkonian M, Villarreal JC, Stevenson DW, Graham SW, Wong GK-S, Mathews S, Pryer KM. 2015b. The origin and evolution of phototropins. *Frontiers in Plant Science* **6**: 637.

Li F-W, Villarreal Aguilar JC, Kelly S, Rothfels CJ, Melkonian M, Frangedakis E, Ruhsam M, Sigel EM, Der JP, Pittermann J *et al.* 2014. Horizontal transfer of an adaptive chimeric photoreceptor from bryophytes to ferns. *Proceedings of the National Academy of Sciences, USA* **111**: 6672–6677.

Li F-W, Villarreal Aguilar JC, Szövényi P. 2017. Hornworts: an overlooked window into carbon-concentrating mechanisms. *Trends in Plant Science* **22**: 275–277.

Ligrone R, Duckett JG, Renzaglia KS. 2012. Major transitions in the evolution of early land plants: a bryological perspective. *Annals of Botany* **109**: 851–871.

Ligrone R, Renzaglia KS. 1990. The sporophyte–gametophyte junction in the hornwort, *Dendroceros tubercularis* Hatt (Anthocerotophyta). *New Phytologist* **114**: 497–505.

Lin Q, Ohashi Y, Kato M, Tsuge T, Gu H, Qu L-J, Aoyama T. 2015. GLABRA2 directly suppresses basic helix-loop-helix transcription factor genes with diverse functions in root hair development. *The Plant Cell* **27**: 2894–2906.

Lindblad P, Bergman B. 2018. The cycad-cyanobacterial symbiosis. In: Rai AN, ed. *CRC handbook of symbiotic cyanobacteria*. Boca Raton, FL, USA: CRC Press, 137–159.

Linde A-M, Eklund DM, Kubota A, Pederson ERA, Holm K, Gyllenstrand N, Nishihama R, Cronberg N, Muranaka T, Oyama T *et al.* 2017. Early evolution of the land plant circadian clock. *New Phytologist* **216**: 576–590.

Liu J-W, Li S-F, Wu C-T, Valdespino IA, Ho J-F, Wu Y-H, Chang H-M, Guu T-Y, Kao M-F, Chesson C *et al.* 2020. Gigantic chloroplasts, including bizonoplasts, are common in shade-adapted species of the ancient vascular plant family Selaginellaceae. *American Journal of Botany* **107**: 562–576.

Liu W, Neal Stewart C. 2015. Plant synthetic biology. *Trends in Plant Science* **20**: 309–317.

Machingura MC, Moroney JV. 2018. Closing the circle. *eLife* **7**: e42507.

Mackinder LCM, Chen C, Leib RD, Patena W, Blum SR, Rodman M, Ramundo S, Adams CM, Jonikas MC. 2017. A spatial interactome reveals the protein organization of the algal CO_2-concentrating mechanism. *Cell* **171**: 133–147.e14.

Mackinder LCM, Meyer MT, Mettler-Altmann T, Chen VK, Mitchell MC, Caspari O, Freeman Rosenzweig ES, Pallesen L, Reeves G, Itakura A *et al.* 2016. A repeat protein links Rubisco to form the eukaryotic carbon-concentrating organelle. *Proceedings of the National Academy of Sciences, USA* **113**: 5958–5963.

Maizel A, Busch MA, Tanahashi T, Perkovic J, Kato M, Hasebe M, Weigel D. 2005. The floral regulator *LEAFY* evolves by substitutions in the DNA binding domain. *Science* **308**: 260–263.

Martin A, Lang D, Hanke ST, Mueller SJX, Sarnighausen E, Vervliet-Scheebaum M, Reski R. 2009. Targeted gene knockouts reveal overlapping functions of the five *Physcomitrella patens* FtsZ isoforms in chloroplast division, chloroplast shaping, cell patterning, plant development, and gravity sensing. *Molecular Plant* **2**: 1359–1372.

Meeks J. 1998. Symbiosis between nitrogen-fixing cyanobacteria and plants. *BioScience* **48**: 266–276.

Meeks JC. 2003. Symbiotic interactions between *Nostoc punctiforme*, a multicellular cyanobacterium, and the hornwort *Anthoceros punctatus*. *Symbiosis* **35**: 55–71.

Menand B, Yi K, Jouannic S, Hoffmann L, Ryan E, Linstead P, Schaefer DG, Dolan L. 2007. An ancient mechanism controls the development of cells with a rooting function in land plants. *Science* **316**: 1477–1480.

Merced A, Renzaglia KS. 2017. Structure, function and evolution of stomata from a bryological perspective. *Bryophyte Diversity and Evolution* **39**: 7.

Merced A, Renzaglia KS. 2019. Contrasting pectin polymers in guard cell walls of *Arabidopsis* and the hornwort *Phaeoceros* reflect physiological differences. *Annals of Botany* **123**: 579–585.

Meyer MT, Whittaker C, Griffiths H. 2017. The algal pyrenoid: key unanswered questions. *Journal of Experimental Botany* **68**: 3739–3749.

Micheli PA. 1927. *Nova plantarum genera*. Florence, Italy: Typis Bernardi Paperinii.

Miwa H, Tamaki T, Fukuda H, Sawa S. 2009. Evolution of CLE signaling: origins of the CLV1 and SOL2/CRN receptor diversity. *Plant Signaling & Behavior* **4**: 477–481.

Moody LA, Kelly S, Rabbinowitsch E, Langdale JA. 2018. Genetic regulation of the 2D to 3D growth transition in the moss *Physcomitrella patens*. *Current Biology* **28**: 473–478.e5.

Morris JL, Puttick MN, Clark JW, Edwards D, Kenrick P, Pressel S, Wellman CH, Yang Z, Schneider H, Donoghue PCJ. 2018. The timescale of early land plant evolution. *Proceedings of the National Academy of Sciences, USA* **115**: E2274–E2283.

Mosquna A, Katz A, Decker EL, Rensing SA, Reski R, Ohad N. 2009. Regulation of stem cell maintenance by the Polycomb protein FIE has been conserved during land plant evolution. *Development* **136**: 2433–2444.

Niklas KJ, Kutschera U. 2009. The evolutionary development of plant body plans. *Functional Plant Biology* **36**: 682.

Nishiyama T, Sakayama H, de Vries J, Buschmann H, Saint-Marcoux D, Ullrich KK, Haas FB, Vanderstraeten L, Becker D, Lang D *et al.* 2018. The *Chara* genome: secondary complexity and implications for plant terrestrialization. *Cell* **174**: 448–464.e24.

Nishiyama T, Wolf PG, Kugita M, Sinclair RB, Sugita M, Sugiura C, Wakasugi T, Yamada K, Yoshinaga K, Yamaguchi K *et al.* 2004. Chloroplast phylogeny indicates that bryophytes are monophyletic. *Molecular Biology and Evolution* **21**: 1813–1819.

Nozue K, Kanegae T, Imaizumi T, Fukuda S, Okamoto H, Yeh KC, Lagarias JC, Wada M. 1998. A phytochrome from the fern *Adiantum* with features of the putative photoreceptor NPH1. *Proceedings of the National Academy of Sciences, USA* **95**: 15826–15830.

Nystedt B, Street NR, Wetterbom A, Zuccolo A, Lin Y-C, Scofield DG, Vezzi F, Delhomme N, Giacomello S, Alexeyenko A *et al.* 2013. The Norway spruce genome sequence and conifer genome evolution. *Nature* **497**: 579–584.

Okano Y, Aono N, Hiwatashi Y, Murata T, Nishiyama T, Ishikawa T, Kubo M, Hasebe M. 2009. A polycomb repressive complex 2 gene regulates apogamy and gives evolutionary insights into early land plant evolution. *Proceedings of the National Academy of Sciences, USA* **106**: 16321–16326.

Okazaki K, Kabeya Y, Miyagishima S-Y. 2010. The evolution of the regulatory mechanism of chloroplast division. *Plant Signaling & Behavior* **5**: 164–167.

Park YI, Chow WS, Anderson JM. 1996. Chloroplast movement in the shade plant *Tradescantia albiflora* helps protect photosystem II against light stress. *Plant Physiology* **111**: 867–875.

Pellicer J, Hidalgo O, Dodsworth S, Leitch IJ. 2018. Genome size diversity and its impact on the evolution of land plants. *Genes* **9**: 88.

Perroud P, Meyberg R, Demko V, Quatrano RS, Olsen O, Rensing SA. 2020. DEK1 displays a strong subcellular polarity during *Physcomitrella patens* 3D growth. *New Phytologist* **226**: 1029–1041.

Pressel S, Renzaglia KS, Dicky Clymo RS, Duckett JG. 2018. Hornwort stomata do not respond actively to exogenous and environmental cues. *Annals of Botany* **122**: 45–57.

Proskauer J. 1948a. Studies on the morphology of *Anthoceros*. II1. *Annals of Botany* **12**: 427–439.

Proskauer J. 1948b. Studies on the morphology of *Anthoceros*. I1. *Annals of Botany* **12**: 237–265.

Proust H, Honkanen S, Jones VAS, Morieri G, Prescott H, Kelly S, Ishizaki K, Kohchi T, Dolan L. 2016. *RSL* Class I genes controlled the development of epidermal structures in the common ancestor of land plants. *Current Biology* **26**: 93–99.

Qiu Y-L, Li L, Wang B, Chen Z, Knoop V, Groth-Malonek M, Dombrovska O, Lee J, Kent L, Rest J *et al.* 2006. The deepest divergences in land plants inferred from phylogenomic evidence. *Proceedings of the National Academy of Sciences, USA* **103**: 15511–15516.

Rai AN, Bergman B, Rasmussen U. 2002. *Cyanobacteria in symbiosis*. Dordrecht, the Netherlands: Kluwer.

Renzaglia KS. 1978. A comparative morphology and developmental anatomy of the Anthocerotophyta. *Journal of the Hattori Botanical Laboratory* **44**: 31–90.

Renzaglia KS, Browning WB, Merced A. 2020. With over 60 independent losses, stomata are expendable in mosses. *Frontiers in Plant Science* **11**: 567.

Renzaglia KS, Duff RJT, Nickrent DL, Garbary DJ. 2000. Vegetative and reproductive innovations of early land plants: implications for a unified phylogeny. *Philosophical Transactions of the Royal Society of London. Series B: Biological Sciences* **355**: 769–793.

Renzaglia KS, Villarreal JC, Duff RJ. 2009. New insights into morphology, anatomy, and systematics of hornworts. In: Goffinet B, Shaw J, eds. *Bryophyte biology*. Cambridge, UK: Cambridge University Press, 139–171.

Renzaglia KS, Villarreal JC, Garbary DJ. 2018. Morphology supports the setaphyte hypothesis: mosses plus liverworts form a natural group. *Bryophyte Diversity and Evolution* **40**: 11.

Renzaglia KS, Villarreal JC, Piatkowski BT, Lucas JR, Merced A. 2017. Hornwort stomata: architecture and fate shared with 400-million-year-old fossil plants without leaves. *Plant Physiology* **174**: 788–797.

Romera-Branchat M, Ripoll JJ, Yanofsky MF, Pelaz S. 2013. The *WOX 13* homeobox gene promotes replum formation in the *Arabidopsis thaliana* fruit. *The Plant Journal* **73**: 37–49.

Sakakibara K, Ando S, Yip HK, Tamada Y, Hiwatashi Y, Murata T, Deguchi H, Hasebe M, Bowman JL. 2013. *KNOX2* genes regulate the haploid-to-diploid morphological transition in land plants. *Science* **339**: 1067–1070.

Sakakibara K, Nishiyama T, Deguchi H, Hasebe M. 2008. Class 1 *KNOX* genes are not involved in shoot development in the moss *Physcomitrella patens* but do function in sporophyte development. *Evolution & Development* **10**: 555–566.

Sakakibara K, Reisewitz P, Aoyama T, Friedrich T, Ando S, Sato Y, Tamada Y, Nishiyama T, Hiwatashi Y, Kurata T *et al.* 2014. *WOX13*-like genes are required for reprogramming of leaf and protoplast cells into stem cells in the moss *Physcomitrella patens*. *Development* **141**: 1660–1670.

Schmitz AJ, Glynn JM, Bradley JS, Stokes KD, Osteryoung KW. 2009. *Arabidopsis FtsZ2-1* and *FtsZ2-2* are functionally redundant, but FtsZbased plastid division is not essential for chloroplast partitioning or plant growth and development. *Molecular Plant* **2**: 1211–1222.

Schneider H, Schuettpelz E, Pryer KM, Cranfill R, Magallón S, Lupia R. 2004. Ferns diversified in the shadow of angiosperms. *Nature* **428**: 553–557.

Shaw J, Renzaglia K. 2004. Phylogeny and diversification of bryophytes. *American Journal of Botany* **91**: 1557–1581.

Shimamura M. 2016. *Marchantia polymorpha*: taxonomy, phylogeny and morphology of a model system. *Plant & Cell Physiology* **57**: 230–256.

Small ID, Schallenberg-Rüdinger M, Takenaka M, Mireau H, Ostersetzer-Biran O. 2019. Plant organellar RNA editing: what 30 years of research has revealed. *The Plant Journal* **101**: 1040–1056.

Söderström L, Hagborg A, von Konrat M, Bartholomew-Began S, Bell D, Briscoe L, Brown E, Cargill DC, Costa DP, Crandall-Stotler BJ *et al.* 2016. World checklist of hornworts and liverworts. *PhytoKeys* **59**: 1–828.

Szövényi P, Frangedakis E, Ricca M, Quandt D, Wicke S, Langdale JA. 2015. Establishment of *Anthoceros agrestis* as a model species for studying the biology of hornworts. *BMC Plant Biology* **15**: 98.

Szövényi P, Waller M, Kirbis A. 2019. Evolution of the plant body plan. *Current Topics in Developmental Biology* **131**: 1–34.

Tam THY, Catarino B, Dolan L. 2015. Conserved regulatory mechanism controls the development of cells with rooting functions in land plants. *Proceedings of the National Academy of Sciences, USA* **112**: E3959–E3968.

Tanahashi T, Sumikawa N, Kato M, Hasebe M. 2005. Diversification of gene function: homologs of the floral regulator FLO/LFY control the first zygotic cell division in the moss *Physcomitrella patens*. *Development* **132**: 1727–1736.

Thamm A, Saunders TE, Dolan L. 2020. MpFEW RHIZOIDS1 miRNA-mediated lateral inhibition controlsrhizoid cell patterning in *Marchantia polymorpha*. *Current Biology: CB* **30**: 1905–1915.e4.

Tillich M, Lehwark P, Morton BR, Maier UG. 2006. The evolution of chloroplast RNA editing. *Molecular Biology and Evolution* **23**: 1912–1921.

Trojan A, Gabrys H. 1996. Chloroplast distribution in *Arabidopsis thaliana* (L.) depends on light conditions during growth. *Plant Physiology* **111**: 419–425.

Ueda M, Zhang Z, Laux T. 2011. Transcriptional activation of *Arabidopsis* axis patterning genes *WOX8/9* links zygote polarity to embryo development. *Developmental Cell* **20**: 264–270.

Vaughn KC, Ligrone R, Owen HA, Hasegawa J, Campbell EO, Renzaglia KS, Monge-Najera J. 1992. The anthocerote chloroplast: a review. *New Phytologist* **120**: 169–190.

Villarreal JC, Cargill DC, Hagborg A, Soderstrom L, Renzaglia KS. 2014. A synthesis of hornwort diversity: patterns, causes and future work. *Phytotaxa* **9**: 150–166.

Villarreal JC, Duckett JG, Pressel S. 2017. Morphology, ultrastructure and phylogenetic affinities of the single-island endemic *Anthoceros cristatus* Steph. (Ascension Island). *Journal of Bryology* **39**: 226–234.

Villarreal JC, Renner SS. 2012. Hornwort pyrenoids, carbon-concentrating structures, evolved and were lost at least five times during the last 100 million years. *Proceedings of the National Academy of Sciences, USA* **109**: 18873–18878.

Villarreal JC, Renner SS. 2013. Correlates of monoicy and dioicy in hornworts, the apparent sister group to vascular plants. *BMC Evolutionary Biology* **13**: 239.

Villarreal JC, Renzaglia KS. 2015. The hornworts: important advancements in early land plant evolution. *Journal of Bryology* **37**: 157–170.

Wada K, Hirabayashi Y, Saito W. 1984. Light germination of *Anthoceros miyabeanus* spores. *The Botanical Magazine Tokyo* **97**: 369–379.

Wang S, Li L, Li H, Sahu SK, Wang H, Xu Y, Xian W, Song B, Liang H, Cheng S *et al.* 2020. Genomes of early-diverging streptophyte algae shed light on plant terrestrialization. *Nature Plants* **6**: 95–106.

Wang Y, Stessman DJ, Spalding MH. 2015. The CO_2 concentrating mechanism and photosynthetic carbon assimilation in limiting CO_2: how *Chlamydomonas* works against the gradient. *The Plant Journal* **82**: 429–448.

Whitewoods CD. 2020. Evolution of CLE peptide signalling. *Seminars in Cell & Developmental Biology*. doi: 10.1016/j.semcdb.2020.04.022.

Whitewoods CD, Cammarata J, Venza ZN, Sang S, Crook AD, Aoyama T, Wang XY, Waller M, Kamisugi Y, Cuming AC *et al.* 2018. CLAVATA was a genetic novelty for the morphological innovation of 3D growth in land plants. *Current Biology* **28**: 2365–2376.e5.

Whitton BA. 1993. Cyanobacteria and Azolla. In: Jones DG, ed. *Exploitation of microorganisms*. Dordrecht, the Netherlands: Springer. 137–167.

Wickett NJ, Mirarab S, Nguyen N, Warnow T, Carpenter E, Matasci N, Ayyampalayam S, Barker MS, Burleigh JG, Gitzendanner MA *et al.* 2014. Phylotranscriptomic analysis of the origin and early diversification of land plants. *Proceedings of the National Academy of Sciences, USA* **111**: E4859–E4868.

Wilhelmsson PKI, Mühlich C, Ullrich KK, Rensing SA. 2017. Comprehensive genome-wide classification reveals that many plant-specific transcription factors evolved in streptophyte algae. *Genome Biology and Evolution* **9**: 3384–3397.

Wilsenach R. 1963. Differentiation of the chloroplast of *Anthoceros*. *The Journal of Cell Biology* **18**: 419–428.

Wu C-C, Li F-W, Kramer EM. 2019. Large-scale phylogenomic analysis suggests three ancient superclades of the WUSCHEL-RELATED HOMEOBOX transcription factor family in plants. *PLoS ONE* **14**: e0223521.

Xiong D, Huang J, Peng S, Li Y. 2017. A few enlarged chloroplasts are less efficient in photosynthesis than a large population of small chloroplasts in *Arabidopsis thaliana*. *Scientific Reports* **7**: 5782.

Xiong W, Fu J, Köllner TG, Chen X, Jia Q, Guo H, Qian P, Guo H, Wu G, Chen F. 2018. Biochemical characterization of microbial type terpene synthases in two closely related species of hornworts, *Anthoceros punctatus* and *Anthoceros agrestis*. *Phytochemistry* **149**: 116–122.

Yamano T, Tsujikawa T, Hatano K, Ozawa S-I, Takahashi Y, Fukuzawa H. 2010. Light and low-CO_2-dependent LCIB-LCIC complex localization in the chloroplast supports the carbon-concentrating mechanism in *Chlamydomonas reinhardtii*. *Plant & Cell Physiology* **51**: 1453–1468.

Zhang J, Fu X-X, Li R-Q, Zhao X, Liu Y, Li M-H, Zwaenepoel A, Ma H, Goffinet B, Guan Y-L *et al.* 2020. The hornwort genome and early land plant evolution. *Nature Plants* **6**: 107–118.

Zhang Y, Jiao Y, Jiao H, Zhao H, Zhu Y-X. 2017. Two-step functional innovation of the stem-cell factors WUS/WOX5 during plant evolution. *Molecular Biology and Evolution* **34**: 640–653.